This is to certify that the
thesis entitled

INVESTIGATIONS ON THE EFFECTS OF CYCLIC LOADING AND THERAPEUTIC TREATMENTS FOLLOWING TRAUMATIC INJURY TO ARTICULAR CARTILAGE

presented by

NURIT GOLENBERG

has been accepted towards fulfillment
of the requirements for the

Master of Science degree in Mechanical Engineering

Roger C. Haut
Major Professor's Signature

August 26, 2009
Date

INVESTIGATIONS ON THE EFFECTS OF CYCLIC LOADING AND THERAPEUTIC TREATMENTS FOLLOWING TRAUMATIC INJURY TO ARTICULAR CARTILAGE

By

Nurit Golenberg

A THESIS

Submitted to
Michigan State University
In partial fulfillment of the requirements
For the degree of

MASTER OF SCIENCE

Mechanical Engineering

2009

ABSTRACT

Investigations on the effects of cyclic loading and therapeutic treatments following traumatic injury to articular cartilage

By

Nurit Golenberg

Osteoarthritis (OA) is a disabling disease of synovial joints, such as the hips and knees, that results in loss of joint function and a reduced quality of life. Joint injuries during sports related activities, specifically anterior cruciate ligament (ACL) tears, greatly increase the risk of developing post-traumatic OA. Since most patients suffering ACL tears develop OA with or without surgical reconstruction of the ligament, the traumatic loads generated on articular cartilage during the acute injury have been suggested to be a major cause of post-traumatic OA. This thesis describes the mechanical and histological properties of the rabbit tibial plateau using the fibril-reinforced biphasic model of cartilage. Additionally, investigation of the mechanical properties and proteoglycan content of bovine chondral explants following two levels of unconfined compressive loading and treatment with a nutraceutical, glucosamine-chondroitin sulfate, has also been described in this thesis. The effect of cyclic loading was evaluated with and without glucosamine chondroitin sulfate treatment following two levels of unconfined compression using bovine chondral explants. The rabbit tibial plateau was again utilized to investigate the long-term effects of P188, a triblock copolymer known to acutely repair damaged cell membranes, following blunt impact to the rabbit tibio-femoral joint. The data presented in this thesis may be used to investigate the progression of the chronic joint disease and introduces possible intervention methods for the prevention of developing OA in the more long term.

Dedication

I would like to thank my parents for their endless love and support throughout my life.

Without their guidance, I would never have dreamed this possible.

Acknowledgments

I would like to thank my advisor and mentor, Dr. Roger Haut, for his guidance and support throughout my research at the Orthopaedics Biomechanics Laboratories. I am extremely grateful to Dr. Wright and Dr. Orth for serving on my committee. I would like to acknowledge Cliff Beckett for his all his technical support. I would also like to acknowledge Jean Atkinson and Jane Walsh for their endless support, hard work and dedication. Finally, I would like to thank my fellow graduate students; Dan Isaac, Tim Baumer, Brian Powell, Eric Meyer, Mark Villwock, Feng Wei, and Jerrod Bramen, for all their help, support, and most importantly their friendship.

Table of Contents

List of Tables

List of Figures

Chapter 1

Background and Literature Review

Osteoarthritis (OA) is a disabling disease of joints, such as the hips and knees, that results in loss of joint function and a reduced quality of life. OA affects almost 27 million Americans each year (Helmick et al. 2008) with a total annual cost per OA patient set at nearly $5700 per year (Maetzel et al., 2004). Injuries during sports related activities, specifically anterior cruciate ligament (ACL) tears, increase the risk of developing OA (Gelber et al., 2000). ACL tears are associated with large compressive forces passing through the joint (Fang et al., 2001). These forces are associated with a significant frequency of occult bone lesions and changes to the overlying articular cartilage homeostasis within 6 months of injury (Vellet et al., 1991; Johnson et al., 1998). Since nearly all patients suffering ACL tears develop OA within 15 years of trauma with or without ACL reconstruction (Myklebust and Bahr, 2005), the traumatic loads to the articular cartilage during injury have been suggested to be the cause of post-traumatic OA.

OA is characterized by increases in cartilage hydration, subchondral bone changes, altered chondrocyte activity, and changes in the structure and composition of proteoglycans and collagen (Mow and Setton, 1998). The process of joint OA involves softening of articular cartilage followed by fibrillation and subsequently, a total loss of the tissue. Because articular cartilage is responsible for the distribution of loads applied to a joint as well as providing a low friction surface for joint movement (Mow et al., 1980),

the loss of articular cartilage ultimately leads to failure of synovial joints (Badley, 2005; Sangha, 2000).

The loss of articular cartilage function can be related to changes in the individual constituents. Articular cartilage is comprised of water (60-80% of tissue's wet weight) and a matrix (20-40% of tissue's wet weight) of cartilage cells or chondrocytes (less than 2%), proteoglycans (PG) (40%) and collagen fibers (60%) (Mow et al., 1980) (Figure 1.1).

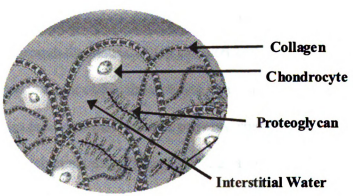

Figure 1.1. Cartilage is comprised of water and a matrix of collagen fibers, chondrocytes, and a proteoglycan complex.

Chondrocytes are responsible for the production and maintenance of the cartilage matrix. Changes in the cell membrane may be responsible for changes in the cellular function. The cell membrane is comprised of a lipid bilayer and protein channels. The membrane and protein channels, such as the Ca+ and Na+/K+ pumps, regulate the ionic and osmotic environment inside the cell. Damage to the membrane or ion channels from excessive compressive loads may cause the cell to lose its ionic and osmotic equilibrium. This results in swelling and overall lysis, a defining feature of necrotic cell death. Traumatic loading to articular cartilage results in apoptotic cell death. Apoptosis results in the fragmentation of the nucleus and eventually cell death. An apoptotic cell contains

apoptotic enzymes that, when released, signal surrounding cells and initiate apoptosis in these cells (Levin et al. 2001). Previous studies have documented cell loss due to traumatic compressive loads and clinically, chondrocyte loss is documented in the cartilage of OA patients; therefore, cell death has been a focus of OA research. Colwell et al. (2001) suggest that it may be possible to limit degeneration and promote repair of the cartilage if cell viability is maintained.

While traumatic loading results in cell death, low level forces can cause changes in the ion channels resulting in increased cellular biosynthesis. Mechanical loads are converted into signals through the matrix which can alter cellular behavior by changing the ionic or osmotic environment of the chondrocyte (Wilkins et al., 2000). The increase in biosynthesis increases the synthesis of matrix proteins, specifically proteoglycans, and therefore increases the mechanical properties of cartilage and its resistance to traumatic overloads (Wei and Haut, 2009).

The matrix, comprised of PGs and collagen, provides cartilage with its compressive resistance to stress and strain overloads. The proteoglycans are comprised of a core protein with glycosaminoglycan (GAG) side chains (Mow and Setton, 1998). These GAG chains have a fixed negative charge that generates a repulsive force causing tension in the cartilage. However, at equilibrium, the swelling pressure due to the PGs is balanced by the forces generated by the collagen. Collagen is a triple helix of polypeptide chains. The orientation of collagen fibers in cartilage is depth dependent. The cartilage is comprised of three layers: the deep zone, middle zone, and superficial zone. The deep zone is roughly the bottom 30% of its thickness. The fibers in this region are perpendicular to the subchondral bone surface. The superficial zone is roughly comprised

of the top 20% of the cartilage thickness. The collagen fibers are tangential to the surface of the cartilage and provide a majority of its tensile properties (Mow et al., 1980) (Figure 1.2). The fibers in the middle or transitional zone, about the middle 50% of the cartilage, are randomly oriented since the fibers are in transition from the deep zone to the superficial zone.

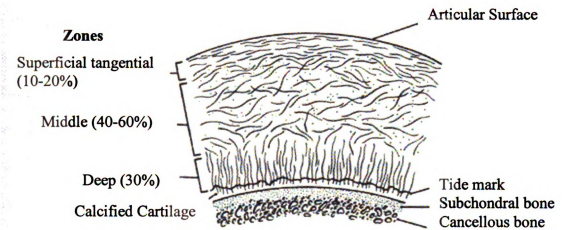

Figure 1.2. The collagen fiber orientation is depth dependent and can be divided into 3 zones. The superficial zone is roughly the top 20% of the cartilage and contains collagen fibers that are tangential to the cartilage surface. The middle zone is roughly the middle 50% of the cartilage and the fibers are oriented randomly. The collagen fibers in the deep zone, bottom 30% are perpendicular to the subchondral bone surface.

Morphological changes, such as fibrillation and tissue swelling, are associated with the initiation of OA. Specifically, fibrillation is due to the unwinding of the collagen fibers and surface fraying. In studies using cartilage explants collagen damage has been observed by surface fissuring (Repo and Finlay, 1997) and the cartilage becomes flattened and elliptical in shape (Jeffrey et al., 1995; Kaab et al., 2000). Additionally, the collagen fibers deform under the compressive loads and, under traumatic loading conditions, the fibers remain in their deformed shape (McCall, 1969). Damage to the

collagen fibers allows the tissue to swell. Swelling of the tissue has been associated with the softening of the tissue. This tissue damage can also be associated with a decrease in the PG content of the tissue (Patwari et al., 2000; Huser and Davies, 2006). This softening, due to fibrillation and swelling, leads to increased pressure on the underlying subchondral bone (Radin et al., 1986; Ewers et al., 2001).

In vivo animal models have been used to study the changes in articular cartilage following both injury and exercise. Our laboratory has previously developed a small animal model to study articular cartilage *in vivo* using Flemish Giant rabbits (Haut et al. 1995). In these previous studies, an impact to the rabbit knee joint results in cartilage surface fissures and decreases in cell viability within 4 days of traumatic injury (Rundell et al., 2005; Isaac et al., 2008) and thickening of the underlying subchondral bone and thinning of the overlying articular cartilage compared to the unimpacted limb 3 years post-trauma (Ewers et al., 2001). On the other hand, exercise increases matrix stiffness and PG content in this tissue. Previous studies using a canine model document an increase in the tissue PG content (Kiveranta et al., 2005), and an increase in its compressive stiffness (Jurvelin et al., 1986) specifically in regions of high loading following regular exercise. A study using a Flemish Giant rabbit model documents that post-traumatic exercise can help prevent the loss of matrix PGs (Weaver and Haut, 2005), but the mechanism of its action was not investigated.

Cartilage explants have also been used to document the changes in the cartilage following compressive loads. A decrease in the cell viability and PG content was documented following traumatic loading and was found to be dependent on load levels and strain rates (Torzilli et al., 1999). Previous studies document that loading above a

critical threshold of 15-20 MPa (Torzilli et al., 1999) causes increased cell death (Phillips and Haut, 2004; Baars et al., 2006; Natoli and Athanasiou, 2008) and permanent damage to the collagen network (Torzilli et al., 1999). Thibault et al. (2002) documents that 40 cycles of 2-8 MPa causes decreased mechanical properties, denatured collagen and loss of PG without producing fissures and cell loss. Cartilage explants have also been used to document the effects of low level loading, below this critical threshold, on both the mechanical and biological properties of the tissue.

Low level mechanical forces applied to cartilage may also cause changes in ion channels of cell membranes. Deformation of the membrane channels may open pathways allowing for changes in the ionic or osmotic environment of the cell, causing changes in cellular metabolism (Wilkins et al., 2000). Single (Torzilli et al., 1999) and cyclic (Wei et al., 2008) low level compression increase PG synthesis in some previous studies. This increase in tissue PG correlates with an increase in tissue stiffness and its resistance to traumatic compression (Wei et al., 2008). Cyclic loading increases the incorporation of nutraceuticals, such as glucosamine-chondroitin sulfate, in the cells (Wei and Haut, 2009, Sharma et al., 2008). Since excessive unconfined compression decreases the PG content of cartilage and decrease its mechanical stiffness pos-trauma, intervention strategies have become a focus of post-traumatic osteoarthritis studies.

Glucosamine and chondroitin sulfate (glcN-CS) have been used in attempts to maintain mechanical properties of injured cartilage in recent years (Wei and Haut, 2009; Sharma et al., 2008, Tiraloche et al., 2005). Glucosamine is a basic building block of proteoglycans (Dodge and Jimenez, 2003), and chondroitin sulfate (CS) increased the synthesis of proteoglycans and hylauronic acid (Morreale et al., 1996). Previous studies,

by others, have shown that bathing cartilage explants in a supplement of glcN-CS can up-regulate the synthesis of tissue PG's (Lippiello, 2003). Therefore, the recovery or prevention of PG loss after trauma with the treatment of glcN-CS has been suggested to maintain the mechanical stiffness of the cartilage and prevent overall loss of this tissue in the joint.

Other pharmaceutical treatments have been investigated to target cell damage and repair. Treatment with poloxamer 188 (P188) has been investigated as a means of repairing the damaged chondrocytes following traumatic injury in hopes of preventing the degeneration of joint cartilage. P188 is an 8400-dalton triblock copolymer containing both hydrophobic and hydrophilic regions, which inserts into only the damaged areas of cell membranes (Marks et al., 2001). Because of its low toxicity, P188 has been used clinically in recent studies following brain trauma. The studies suggest that P188 can help 'save' neurons from developing early necrotic death following severe mechanical loading (Barbee et al., 1992; Marks et al., 2001). Acute studies have been conducted recently to determine the efficacy of P188 in repairing damaged cell membranes following traumatic injury to articular cartilage. Specifically, Rundell et al. (2005), using the patello-femoral joint, and Isaac et al. (In Review), using the tibio-femoral joint, have documented increases in the percentage of viable cells in impacted limbs treated with P188 up to 4 days following a traumatic overloading of the joint. Similarly, *in vitro* studies have documented the ability of P188 to acutely repair damaged membranes in chondrocytes 7 days after a traumatic overload (Baars et al., 2006; Phillips and Haut, 2004; Natoli and Athanasiou, 2008). These results suggest that P188 may provide a possible treatment for

the prevention of post-trauma induced OA of the joint. However, the long term efficacy of P188 and the effect of saving these cells is yet unknown in the current literature.

To study the effects of the degenerative changes in joint cartilage, various computational models, such as the linear elastic and linear biphasic models of cartilage, have been developed to extract the mechanical properties from creep and indentation-relaxation tests. These tests have been used to extract properties initially and at equilibrium. Specifically, the linear elastic model has been used to determine the instantaneous and equilibrium modulii after assuming Poisson's ratio of the tissue (Parsons and Black, 1977). More recently, Jin and Lewis (2004) have developed a two-punch test to extract the effective Poisson's ratio of the tissue. The linear elastic model, however, is limited in evaluating the mechanical properties only under small loads and small strains. The model also does not incorporate the fluid flow characteristics of the tissue. On the other hand, the linear biphasic model has been used to study changes in the linear elastic equilibrium modulus, Poisson's ratio, and the tissue permeability of cartilage (Mow et al. 1980). Yet, it is unable to evaluate the instantaneous response of the cartilage to a compressive load. The limitations of these models have resulted in numerous inconsistencies in the data. For example, using the linear biphasic model on the rabbit tibial plateau, a previous study documents a lower aggregate modulus, extracted from the equilibrium data, on the medial than lateral facet in areas covered by the meniscus (Roemhildt et al. 2006). In contrast to these findings, a previous study using the linear elastic model, suggested a higher creep modulus in medial compared to lateral facet in regions partially covered by the meniscus in the rabbit tibial plateau (Rasanen and Messner, 1996; Wei, Rasanen, and Messner, 1998). The instantaneous properties

correlate with the integrity of the collagen matrix while the equilibrium properties correlate with the network of proteoglycans (Julkunen et al., 2009). The content of proteoglycans is inversely proportional to tissue permeability (Maroudas, 1979). The correlations between morphological and mechanical properties of cartilage have often been confusing and contradictory possible because of limitations in the computational models. For example, using the linear biphasic model the equilibrium modulus and Poisson's ratio were found to be lower in the medial versus lateral compartment of the tibial plateau (Roemhildt et al., 2006). The equilibrium modulus is consistent with previous findings that suggest the medial compartment to be more degraded with slightly rougher surfaces and/or the presence of superficial or deep splits. These morphological results suggest that the collagen network in cartilage from the medial compartment of the rabbit tibial plateau may be more degraded than in the lateral compartment (Pelletier et al., 1983; Bank et al., 2000) and that Poisson's ratio should be larger in that compartment (Kiviranta et al., 2006). Recent studies suggest that a more complex model of cartilage, which incorporates a collagen fiber network within the matrix, may more accurately fit the creep and relaxation response of cartilage under unconfined and confined compression as well as indentation testing (Wilson et al. 2005), and therefore better correlate with histological and morphological data. The fibril-reinforced biphasic model incorporates both the instantaneous and equilibrium parameters as well as the tissue permeability and can evaluate these parameters using a single indentation test. However, little information using this model has currently been documented.

This thesis describes investigations on articular cartilage in both *in vivo* and *in vitro* scenarios using a previously established rabbit model and bovine chondral explants,

respectively. Using the fibril-reinforced biphasic model of cartilage, Chapter 2 will document the mechanical properties of the rabbit tibial plateau in the medial and lateral facets in areas covered and uncovered by the meniscus. Histological and morphological characteristics of the tibial plateau cartilage were documented and correlated with the mechanical properties generated in the model. Chapter 3 will investigate the mechanical properties of bovine chondral explants following 10 MPa and 25 MPa of unconfined compression. Additionally, treatment of the explants with glcN-CS following unconfined compression will be investigated. Using this model Chapter 4 will investigate the effect of low level cyclic loading post-trauma on the chondral explants. GlcN-CS incorporation will also be investigated following low level cyclic loading on the injured cartilage explants. In Chapter 5, cell viability analysis is used to investigate the long term efficacy of a single injection of P188 to 'save' cells in the rabbit TF joint following a single traumatic impact to the joint.

References

Baars, D.C., Rundell, S.A., Haut, R.C. (2006) Treatment with the non-ionic surfactant poloxamer P188 reduces DNA fragmentation in cells from bovine chondral explants exposed to injurious unconfined compression. *Biomech Model Mechanobiol* **5,** 133-139.

Badley, E.M. (2005) The impact of disabling arthritis. *Arthritis and Rheumatism* **8,** 221-228.

Bank, R.A., Soudry, M., Maroudas, A., Mizrahi, J., and TeKoppele, J.M. (2000) The increased swelling and instantaneous deformation of osteoarthritic cartilage is highly correlated with collagen degradation. *Arthritis and Rheumatism* **43,** 2202-2210.

Barbee, K., Ford, C., Blackman, B., Thibault, L. (1992) Neural cell injury: characterization and treatment strategy In 2nd Injury Prevention Through Biomechanics Symposium Proceeding, CDC. Edited by Yang K.

Colwell, C.W., D'Lima, D.D., Hoenecke, H.R., Fronek, J., Pulido, P., Morris, B.A., Chung, C., Resnick, D., Lotz, M. (2001) In vivo changes after mechanical injury. *Clin. Orthop. Rel. Res.* **391S,** S116-S123.

Dodge, G.R. and Jimenez, S.A. (2003) Glucosamine sulfate modulates the levels of aggrecan and matrix metalloproteinase-3 synthesized by cultured human osteoarthritis articular chondrocytes. *Osteoarthritis and Cartilage* **11,** 424-432.

Ewers, B.J., Weaver, B.T., Sevensma, E.T., Haut, R.C., (2001) Chronic changes in rabbit retro-patellar cartilage and subchondral bone after blunt impact loading of the patellofemoral joint. *Journal of Orthopaedic Research* **20,** 545-550.

Fang, C., Johnson, D., Leslie, M.P., Carlson, C.S., Robbins, M., Di Cesare, P.E. (2001) Tissue distribution and measurement of cartilage oligomeric matrix protein in patients with magnetic resonance imaging-detected bone bruises after acute anterior cruiate ligament tears. *Journal of Orthopaedic Research* **19,** 634-641.

Gelber, A.C., Hochberg, M.C., Mead, L.A., Wang, N-Y., Wigley, F.M., Klag, M.J., (2000) Joint injury in young adults and risk for subsequent knee and hip osteoarthritis. *Annals of Internal Medicine* **133,** 321-328.

Haut, R.C., Ide, T.M., and DeCamp, C.E. (1995) Mechanical responses of the rabbit petello-femoral joint to blunt impact. *Journal of Biomechanical Engineering* **117,** 402-408.

Helmick, C.G., Felson, D.T, Lawrence, R.C., Gabriel, S., Hirch, R., Kwoh, C.K., Liang, M.H., Kremers, H.M., Mayes, M.D., Merkel, P.A., Pillemer, S.R., Reveille, J.D., Stone, J.H. (2008) Estimates of the prevalence of arthritis and other rheumatic conditions in the United States. *Arthritis and Rheumatism* **58,** 15-25.

Huser, C.A.M., Davies, M.E. (2006) Validation of an in vitro single-impact load model of the initiation of osteoarthritis-like changes in articular cartilage. *Journal of Orthopaedic Research* **24**, 725-732.

Isaac, D.I., Golenberg, N., Haut, R.C. Acute repair of chondrocytes in the rabbit tibiofemoral joint following blunt impact using P188 surfactant and a preliminary investigation of its long-term efficacy. *Journal of Orthopaedic Research* (In Review).

Isaac, D.I., Meyer, E.G., Haut, R.C. (2008) Chondrocyte damage and contact pressures following impact on the rabbit tibiofemoral joint. *J Biomech Eng* **130,** 0410181-5.

Jeffrey, J.E., Gregory, D.W., Aspden, R.M. (1995) Matrix damage and chondrocyte viability following a single impact load on articular cartilage. *Archives of Biochemistry and Biophysics* **322**, 87-96.

Jin, H. and Lewis, J.L. (2004) Determination of Poisson's ratio of articular cartilage by indentation using different-sized indenters. *Journal of Biomechanical Engineering* **126,** 138-145.

Johnson, D.L., Urban, W.P., Caborn, D.N.M., Vanarthos, W.J., Carlson, C.S. (1998) Articular cartilage changes seen with magnetic resonance imagine-detected bone bruises associated with acute anterior cruciate ligament rupture. *The American Journal of Sports Medicine* **26**, 409-414.

Julkunen, P., Harjula, T., Marjanen, J., Helminen, H.J., Jurvelin, J.S. (2009) Comparison of single-phase isotropic elastic and fibril-reinforced poroelastic models for indentation of rabbit articular cartilage. *Journal of Biomechanics* **42**, 652-656.

Jurvelin, J., Kiviranta, I., Tammi, M., Helminen, H.J., (1986) Effect of physical exercise on indentation stiffness of articular cartilage in the canine knee. *Int. J. Sports Med.* **7**, 106-110.

Kaab M.J., Ito, K., Rahn, B., Clark, J.M., Notzli, H.P. (2000) Effect of mechanical load on articular cartilage collagen structure: a scanning electron-microscope study. *Cells Tissues Organs* **167**, 106-120.

Kiviranta, P., Rieppo, R.K., Julunen, P., Toyras, J., and Jurvelin, J.S. (2006) Collagen network primarily controls Poisson's ratio of bovine articular cartilage in compression. *Journal of Orthopaedic Research* **24**, 690-699.

Levin, A., Burton-Wurster, N., Chen, C.T., Lust, G. (2001) Intercellular signaling as a cause of cell death in cyclically impacted cartilage explants. *Osteoarthritis and Cartilage* **9**, 702-711.

Lippiello, L. (2003) Glucosamine and chondroitin sulfate: biological response modifiers of chondrocytes under simulated conditions of joint stress. *OsteoArthritis and Cartilage* **11**, 335-342.

Maetzel, A., Li, L.C., Pencharz, J., Tomlinson, G., Bombardier, C. (2004) The economic burden associated with osteoarthritis, rheumatoid arthritis, and hypertension: a comparative study. *Annals of the Rheumatic Diseases* **63**, 395-401.

Marks, J.D., Pan, C.Y., Bushell, T., Cromie, W., Lee, R.C. (2001) Amphiphilic tri-block copolymers provide potent membrane-targeted neuroprotection. *FASEB* **15**, 1107-1109.

Maroudas, A. (1979) A physical properties of articular cartilage. In: Freeman, M.A.R. (ed) *Adult articular cartilage*. Kent, NY: Pitman medical, 215-290.

McCall, J.G. (1969) Load-deformation studies of articular cartilage. *Journal of Anatomy* **105**, 212-214.

Morreale, P., Manopulo, R., Galati, M., Boccanera, L., Saponati, G., Bocchi, L. (1996) Comparison of anti-inflammatory efficacy of chondroitin sulfate and diclofenac sodium in patients with knee osteoarthritis. *Journal of Rheumatology* **23**, 1385-1391.

Mow, V.C., Roth, V., Armstrong, C.G. (1980) Biomechanics of joint cartilage. In: Frankel, V.H., Nordin, M. (eds) *Basic Biomechanics of the Skeletal System.* Philadelphia, PA: Lea & Febiger, 63-85.

Mow, V.C. and Setton, L.A. (1998) Mechanical properties of normal and osteoarthiric cartilage. In: Brandt, K.D., Doherty, M., Lohmander, L.S., (eds). *Osteoarthritis.* Oxford: Oxford University Press, 108-122.

Myklebust, G. and Bahr, R. (2005) Return to play guidelines after anterior cruciate ligament surgery. *British Journal of Sports Medicine* **39**, 127-131.

Natoli, R.M., Athanasiou, K.A. (2008) P188 reduces cell death and IGF-I reduces GAG release following single-impact loading of articular cartilage. *J Biomech Eng* **130**, 041012-1-9.

Parsons, J.R. and Black, J. (1977) The viscoelastic shear behavior of normal rabbit articular cartilage. *Journal of Biomechanics* **10**, 21-29.

Patwari, P., Kurz, B., Sandy, J.D., Grodzinsky, A.J., (2000) Mannosamine inhibits aggrecanase-mediated changes in physical properties and biochemical composition of articular cartilage. *Archives of Biochemistry and Biophysics* **374**, 79-85.

Pelletier, J.P., Martel-Palletier, J., Altman, R.D., Ghandur/Mnaymneh, L., Hower, D.S., and Woessner, J.F., (1983) Collagenolytic activity and collagen matrix breakdown of the articular cartilage in de Pond-Nuki dog model of osteoarthritis. *Arthritis and Rheumatism* **26**, 866-874.

Phillips, D.M. and Haut, R.C. (2004) The use of non-ionic surfactant (P188) to save chondrocytes from necrosis following impact loading of chondral explants. *Journal of Orthopaedic Research* **22**, 1135-1142.

Radin, E., Rose, R. (1986) Role of Subchondral Bone in the Initiation and Progression of Cartilage Damage. *Clin Orthop Rel Res* **213**, 34-40.

Rasanen, T. and Messner, K. (1996) Regional variations of indentation stiffness and thickness of normal rabbit knee articular cartilage. *Journal of Biomedical Materials Research* **31**, 519-524.

Repo, R.U., Finlay, J.B. (1977) Survival of articular cartilage after controlled impact. *Journal of Bone and Joint Surgery-American Volume* **59**, 1068-1076.

Roemhildt, M.L., Coughlin, K.M., Peura, G.D., Fleming, B.C., and Beynnon, B.D. (2006) Material properties of articular cartilage in the rabbit tibial plateau. *Journal of Biomechanics* **39**, 2331-2337.

Rundell, S.A., Baars, D.C, Phillips, D.M., Haut, R.C. (2005) The limitation of acute necrosis in retro-patellar cartilage after a severe blunt impact to the in vivo rabbit patellofemoral joint. *Journal of Orthopaedic Research* **23**, 1363-1369.

Sangha, O. (2000) Epidemiology of rheumatic diseases. *Rheumatology* **39**, 3-12.

Sharma, G., Sazena, R.K., Mishra, P. (2008) Synergistic effect of chondroitin sulfate and cyclic pressure on biochemical and morphological properties of chondrocytes from articular cartilage. *Osteoarthritis and Cartilage* **16**, 1387-1394.

Thibault, M., Poole, A.R., Buschmann, M.D. (2002) Cyclic compression of cartilage/bone explants in vitro leads to physical weakening, mechanical breakdown of collagen and release of matrix fragments. *Journal of Orthopaedic Research* **20**, 1265-1273.

Torzilli, P.A., Grigiene, R., Borrelli, J. Jr., Helfet, D.L. (1999) Effect of impact load on articular cartilage: cell metabolism and viability, and matrix water content. *Journal of Biomechanical Engineering* **121**, 433-441.

Vellet, A.D., Marks, P.H., Fowler, P.J., Munro, T.G. (1991) Occult posttraumatic osteochondral lesions of the knee: prevalence, classification and short-term sequelae evaluated with MR imagining. *Radiology* **178**, 271-276.

Weaver, B.T. and Haut, R.C. (2005) Enforced Exercise after blunt trauma significantly affects biomechanical and histological changes in rabbit retro-patellar cartilage. *Journal of Biomechanics* **38**, 1177-1183.

Wei, X., Rasanen, T., and Messner, K. (1998) Maturation-related compressive properties of rabbit knee articular cartilage and volume fraction of subchondral tissue. *Osteoarthritis and Cartilage* **6**, 400-409.

Wei, F., Golenberg, N., Kepich, E.T., Haut, R.C. (2008) Effect of intermittent cyclic preloads on the response of articular cartilage explants to an excessive level of unconfined compression. *Journal of Orthopaedic Research* **26**, 1636-1642.

Wei, F. and Haut, R.C. (2009) High levels of glucosamine-chondroitin sulfate can alter the cyclic preload and acute overload responses of chondral explants. *Journal of Orthopaedic Research* **27**, 353-359.

Wilkins, R.J., Browning, J.A., Urban, J.P.G. (2000) Chondrocyte regulation by mechanical load. *Bioheology* **37**, 67-74.

Wilson, W., van Donkelaar, C.C., van Rietbergen, B., and Huiskes, R. (2005) 'A fibril-reinforced poroviscoelastic swelling model for articular cartilage', *Journal of Biomechanics* **38**, 1195-1204.

Chapter 2

Histomorphological and mechanical property correlations in rabbit tibial plateau cartilage based on a fibril-reinforced biphasic model

Abstract

The rabbit knee joint has frequently been used to study the mechanical properties of articular cartilage using various computational models. These models, however, vary in their ability to extract comparable material properties of cartilage from experimental data, resulting in inconsistencies in the data from various laboratories. A more complex, fibril-reinforced biphasic model more accurately fits the response of the cartilage by incorporating a collagen fiber network within the matrix. Indentation-relaxation tests were conducted on the medial and lateral facets in areas covered and uncovered by the meniscus on the rabbit tibial plateau. Gross and histological data were analyzed and correlated with the mechanical properties. The fibril-reinforced biphasic model accurately fit the entire experimental curve extracting both the instantaneous (fiber modulus) and equilibrium (matrix modulus) responses, and tissue permeability. The data was found significant at all sites. Significant correlations were also documented between the mechanical and the histological and morphological data.

Introduction

The rabbit knee joint has frequently been used as a model to study the mechanical properties of articular cartilage (Wei et al., 1998; Roemhildt et al., 2006). The model has also been used to better understand the development of joint disease, such as osteoarthritis (OA), resulting from traumatic injury (Ewers et al., 2002), knee joint instability (Sah et al., 1997; Vignon et al., 1987; Mansour et al., 1998), and meniscectomy (Hoch et al., 1983).

To determine the changes that occur in the mechanical properties of articular cartilage in the above studies, various computational models of cartilage have been utilized to analyze the experimental data. In situ indentation tests have, for the most part, been the experiment of choice to extract the material characteristics of cartilage, largely because the method preserves the structural integrity of the tissue on the joint surface (Sah et al. 1997; Mow et al. 1980). Various types of computational models may vary, however, in their ability to extract comparable material properties of cartilage from experimental data. Consequently, correlations between mechanical properties and the histological or morphological characteristics of cartilage tissue from different laboratories can be confusing or even contradictory.

The linear elastic model of articular cartilage was one of the first to be used in order to reduce experimental indentation test data (Hayes et al., 1972). Theoretically, this model is appropriate under small loads associated with small strain assumptions, but various studies have utilized the model for 20% strain (Haut et al., 1995). The model analysis has also been modified to account for non-linear geometric effects (Zhang et al., 1997). Typically this model is used in relaxation and creep tests to extract the compressive moduli of cartilage either instantly by assuming Poisson's ratio to be 0.5, or

at equilibrium where the ratio is assumed to be 0.4 (Parsons and Black, 1977). More recently, a 2-punch test has been developed in an attempt to extract the effective Poisson's ratio from this elastic model (Jin and Lewis, 2004). The model has also been used to estimate the relaxation and creep characteristics of cartilage by using an associated linear viscoelastic solution (Jurvelin et al., 1990). Using the elastic model, Hoch et al. (1983), for example, document that the equilibrium compressive modulus of articular cartilage on the rabbit tibial plateau in central areas not covered by meniscus is slightly higher on the medial than lateral facet. Similarly, using the same model, Rasanen and Messner (1996) document a creep modulus after 15 sec. in the central partially covered area of the rabbit plateau to be slightly higher on the medial than lateral facet. In the same study a so called "ramp Young's modulus" is also documented at the 200 millisecond time point to be higher on the medial than lateral facet. These investigators hypothesize that the *in vivo* stresses on the medial facet are likely higher than on the lateral facet, possibly due to higher loading pressures (Kempson, 1979; Swann and Seedhom, 1986). This hypothesis, however, is in contrast to more recent experimental data in which the investigators suggest that contact loads on the lateral facet may often be greater than on the medial facet during hopping gait (Gushue et al., 2005). Wei et al. (1998) also use the linear elastic model to determine the instantaneous (at 200 ms) and 50-second creep modulus of cartilage centrally located on the rabbit tibial plateau. A Poisson's ratio of 0.3 is used for the calculation of 50 sec. creep modulus, based on the literature, in this study. The investigators document a higher instantaneous modulus on the lateral than medial facet, which is inconsistent with previous findings by Rasanen and Messner (1996). On the other hand, the 50-sec

modulus is slightly higher medial than lateral from the study, which is in support of Rasanen and Messner's findings. However, this notion is in contrast with the ideas presented by Gushue et al., (2005).

The linear biphasic model of cartilage is able to determine the linearly elastic equilibrium modulus and Poisson's ratio of the matrix, as well as the tissue permeability directly from experimental creep or relaxation data (Mow et al.1980). On the other hand, the model does not include a parameter that directly relates to the instantaneous response of the tissue. A recent study by Roemhildt et al. (2006) utilizes the linear biphasic model to extract the material properties of rabbit articular cartilage across the tibial plateau from creep indentation data. The investigators document that the aggregate modulus, extracted from equilibrium data, is slightly lower medially than laterally in posterior areas of the plateau covered by meniscus. This is in contrast with the findings that suggest a higher creep modulus in areas partially covered by the meniscus documented using the linear elastic model (Rasanen and Messner, 1996; Wei et al., 1998). No significant differences, however, were noted medial to lateral in the uncovered areas of the plateau. The study also determines that Poisson's ratio is smaller on the medial than lateral facets, and the permeability of cartilage on the medial facet is significantly greater than on the lateral facet. The result is consistent with the observation that "the medial compartments had slightly rougher surfaces and/or the presence of superficial or deep splits." These morphological results, on the other hand, suggest that the collagen network in cartilage from the medial compartment of the rabbit tibial plateau may be more degraded than in the lateral compartment (Pelletier et al., 1983; Bank et al., 2000). Yet a more degraded collagen network in the medial than lateral compartment suggests

that Poisson's ratio in the medial compartment may be greater than in the lateral compartment, per a recent study by Kiviranta et al., (2006), using a fibril-reinforced biphasic model for cartilage. Recent studies in the literature suggest that this more complex model of cartilage, which incorporates a collagen fiber network within the matrix, may more accurately fit the creep and relaxation responses of cartilage under both unconfined and confined compression, as well as indentation testing (Wilson et al., 2005).

The objective of the current study was to document the mechanical properties of articular cartilage in meniscal covered and uncovered areas of the rabbit tibial plateau using the fibril-reinforced poroelastic model for the tissue. Both the histological and morphological characteristics were also documented across the tibial plateau in an attempt to show that the model could provide material properties across the plateau that were consistent with histological and morphological data, as well as to compare data from earlier studies that have utilized less complex models of articular cartilage for extraction of the material properties from indentation test data.

Methods

A total of 10 Flemish Giant rabbits (4.5 +/- 0.7 kg, 6-8 months of age) were used in the study. This study was approved by an All-University Committee on Animal Use and Care. The rabbits were exercised 10 min. per day on a treadmill at a speed of 0.3 mph, 5 days a week for this 12 month study (Oyen-Tiesma et al., 1998). A single licensed veterinary technician (J.A.) conducted all exercise sessions.

After 12 months, the animals were sacrificed with Pentobarbital (85.9 mg/kg body weight). The hind limbs were opened and examined for gross abnormalities, such as advanced joint disease or inflammation in the joint. The meniscus was also examined, and it was removed after marking its location on the tibial plateau. The surfaces were stained with India ink and the length of surface fissures was measured from a digital photograph (Polaroid DMC2, Polaroid Corp., Waltham, MA) taken under a dissecting microscope (Wild TYP 374590, Heerbrugg, Switzerland), by a single observer (E.M.) using image analysis software (SigmaScan, SPSS Inc., Chicago, IL). The mechanical properties of articular cartilage were documented at four sites across the medial and lateral facets of the tibial plateau using indentation relaxation tests (Haut et al., 1995). The sites were near the edge of the meniscus on the medial (Site 1) and lateral (Site 3) facets in uncovered areas (Figure 2.1). Sites 2 and 4 were slightly posterior and under the medial and lateral meniscus, respectively.

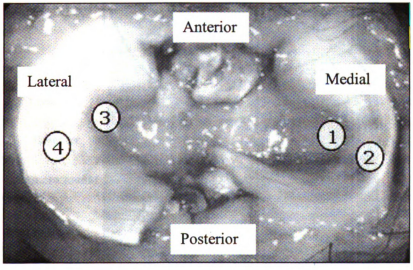

Figure 2.1. Indentation relaxation test sites located on the rabbit tibial plateau. Sites 1 and 3 correspond to the areas not covered by the meniscus on the medial and lateral facets, respectively. Sites 2 (medial) and 4 (lateral) are the areas covered by the meniscus.

The tibial plateau was cut from the tibia and was mounted in a clamp which was bathed in room temperature phosphate buffered saline for mechanical tests. At each site the surface of the plateau was adjusted to be perpendicular to the indenter probe with a camera mount (model 3265, Bogen Manfrotto, Italy). After a preload of 0.03N was applied, a 1 mm diameter, flat non-porous probe was then pressed into the cartilage 0.1 mm in 30 ms and maintained for 150 s using a custom-built stepper motor device (Physic Instruments, Waldbronn, Germany, Model M-168.3) (Figure 2.2). The resistive loads were measured (Data Instruments, Acton MA, Model JP-25), amplified, and sampled at 1000 Hz for the first second and 20 Hz thereafter. After 5 minutes of rest, a needle probe was pressed into the cartilage to measure thickness (Athanasiou et al., 1991).

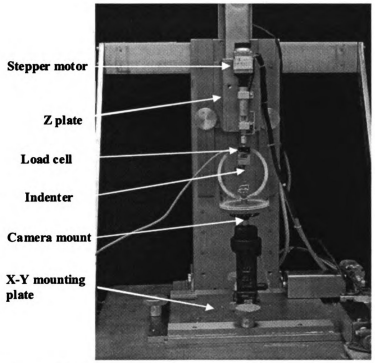

Figure 2.2. Photograph of the indentation test fixture. The X-Y mounting plate allows for left/right or forward/backward placement, and the Z plate allows for up.down placement. The camera mount allowed for rotation of the sample to set the surface perpendicular to the indenter.

The mechanical tests were simulated with a fibril-reinforced biphasic cartilage model (Li et al., 1999) and implemented in a finite element package (Abaqus v.6.3, Hibbitt, Karlsson & Sorensen, Inc., Pawtucket, RI, USA). A compressible neo-Hookean material with Young's modulus E_m and an assumed Poisson's ratio (ν_m=0.3) were assigned to the non-fibrillar part of the matrix.

The fiber network was modeled as non-linear springs with Young's modulus given by

$$E_f = w(z,h)E_\varepsilon \varepsilon_f, \;\; \varepsilon_f \geq 0, \;\; 0 \leq z \leq h, \tag{1}$$

where E_ε was an elastic modulus parameter for the fibers, ε_f was the strain in the fiber direction, $w(z)$ was a non-dimensional weight function, and h was the tissue thickness. To account for the mainly horizontal collagen fiber distribution in the superficial zone, a weight function was defined (Li et al., 2000):

$$w(z,h) = \begin{cases} -\dfrac{25}{16}\left(\dfrac{z}{h}\right)^2 + \dfrac{40}{16}\dfrac{z}{h}, & \dfrac{z}{h} \in [0,0.8] \\ 1, & \dfrac{z}{h} \in (0.8,0.1] \end{cases} \tag{2}$$

Permeability of the tissue (k) was assumed to be strain dependent (van der Voet, 1997):

$$k = k_0\left(\frac{1+e}{1+e_0}\right)^M, \tag{3}$$

Where k_0 was the initial permeability, M was a stiffening constant, and e and e_0 were the current and initial void ratios, respectively. Initial water content was assumed to be linearly decreasing from 85% superficially to 70% at the cartilage-bone interface (Lipshitz et al., 1975).

For simulation, the axisymmetric finite element mesh consisted of pore pressure elements (model type CAX4P) for the matrix, and nonlinear spring elements (model type SPRINGA) for the fibers. The specimen was modeled as a circular disc with radius of 4 mm. The bottom nodes where fixed to simulate attachment to underlying bone. The indenter was modeled as rigid, frictionless and non-permeable. To specify unrestricted fluid flow out of the tissue, zero pore pressure was prescribed at the top nodes outside the indenter and at the outer boundary. The mesh consisted of 64 elements in the radial direction and 18-26 elements in the vertical direction, depending on the specimen thickness. In preliminary studies by this lab (not published), mesh sensitivity analyses were conducted on the finite-element model in order to optimize its rate of convergence for typical model parameters.

To optimize agreement between experimental data and the numerical simulations, a custom-written Gauss-Newton constrained nonlinear least-squares minimization procedure was used in an iterative fashion (Lindstrom and Wedin, 1993). Sensitivity analysis was performed for the four unknown material parameters (E_m, E_ε, k_0, and M) to ensure that the constants were uniquely identifiable from a single indentation experiment. The dimensionless sensitivity coefficients were defined as

$$\chi_f(\beta_i) = \frac{\beta_{i0}}{f_{\max}} \frac{\partial f}{\partial \beta_i}, \quad (4)$$

where β_i is the i-th parameter, β_{i0} is its nominal value, $f(\beta_1, \beta_2, \ldots \beta_n)$ is a state variable (reaction force), and $f_{\max}$ is its maximum value (Beck et al., 1977). It was assumed that the experimental data were sensitive to a particular parameter when $|\chi_f(\beta_i)| > 0.1$. To ensure uniqueness of each parameter, the sensitivity plots were checked for linear independence over time.

After mechanical tests, the specimen was placed in 10% buffered formalin and decalcified in 20% formic acid. Coronal-oriented tissue blocks were cut from the plateau. The blocks were processed in paraffin and six sequential sections, 8 microns thick, were stained with Safranin O-Fast Green and examined under light microscopy. The thicknesses of articular cartilage, the zone of calcified cartilage and subchondral bone were determined by averaging across each facet with a calibrated eyepiece by 3 readers (EH, EM, JW). The readers also scored various histological parameters from the articular cartilage and zone of calcified cartilage using an established scoring system (Figure 2.3) (Weaver and Haut, 2005; Columbo et al., 1983; Mazieres et al., 1987).

Articular Cartilage Fissures			**Articular Cartilage Disruptions**		
	None	0		None	0
	1-3 Surface	1		Compression Ridges	2
	1-2 Midzone	2		Horizontal Splits	4
	3-4 Midzone	3		Vertical Splits	4
	4+ Midzone	4			
	1+ Deep Zone	4			
Proteoglycan Stain			**Calcified Cartilage Stain**		
	Normal	0		Normal	0
	Slight Loss	1		Slight	1
	Moderate Loss	2		Moderate	2
	Focally Total Loss	3 4		Dark	3

Figure 2.3. Histomorphometric scoring system used to quantify the characteristics for cartilage across the tibial plateau.

The mechanical testing and thickness data from the right and left limbs of each animal were compared using t-tests. The limb-averaged data was subjected to a two factor (medial/lateral location; covered/uncovered) repeated (both factors) measures ANOVA with post hoc Student-Newman-Keuls (S-N-K) tests. Non-parametric statistical tests were used for the ordinal histological data analyses. Friedman, repeated measures ANOVA on ranks was used for the analysis of differences between readers. Kruskal-Wallis single factor ANOVA on Ranks with S-N-K post hoc testing was used to test for differences between the right and left limbs. Wilcoxon Signed Rank tests and S-N-K post hoc tests were used to test for differences between medial and lateral facets. Spearman correlations were conducted on the mechanical and histomorphological data. A significant statistical effect was indicated for $p < 0.05$.

Results

Gross examination of the joints indicated no signs of joint disease. India ink staining of the plateau indicated surface irregularities and fissures on both facets (Figure 2.4). There was no difference in the length of the surface fissures on right versus left limbs. The length of the fissures on the medial facet (72.6 ± 21.6 mm) was significantly greater than on the lateral facet (54.8 ± 10.0 mm).

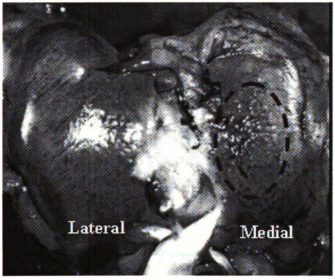

Figure 2.4. Gross photographs of the tibial surface, stained with India ink to highlight fissures. Surface irregularities were analyzed, comparing the medial and lateral facets.

Indentation relaxation testing on the tibial plateau indicated a high frequency load response immediately after the probe was stopped. This led to a difficulty in determining the time at "peak load". Therefore, this time point was determined by a linear interpolation of the load data in the vicinity of this peak. The latter was used in the finite element simulation of the indentation test in the optimization process. In all cases the theoretical curves, with optimized parameters, closely fit the experimental data (Figure 2.5).

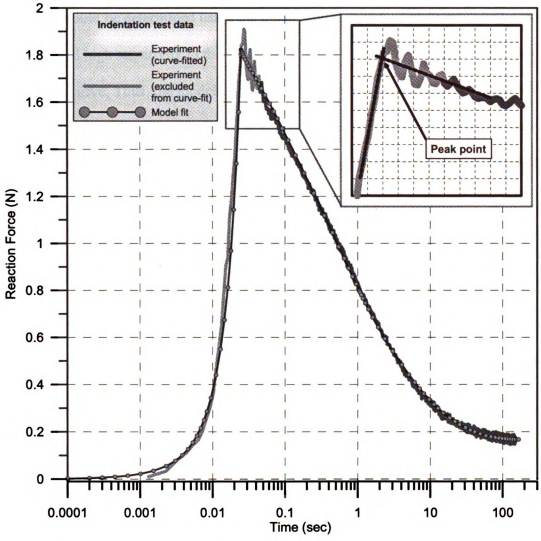

Figure 2.5. Theoretical curves were calculated to closely fit the data collected during experimental testing.

A sensitivity plot for typical values of the material parameters (E_m, E_ε, k_0, and M) indicated that the response curves were highly sensitive to the matrix and fiber modulus, as well as for k_o and M (Figure 2.6a). All parameters were also linearly independent from one another, as indicated by the very distinct shape of each sensitivity curve. This plot demonstrated that the peak load response was very sensitive to the value of fiber modulus near the time of peak load, which is the time when the instantaneous

modulus would be determined using the linear elastic model. The experimental curves also showed high sensitivity to the value of the matrix modulus throughout the entire relaxation curve. Thus, the model parameter was determined to coincide closely with values of the equilibrium modulus from the linear elastic theory. The response during the transition from the peak load to equilibrium was sensitive to the value of permeability and the stiffening parameter. Yet, during the curve fitting process the values of the stiffening parameter and permeability at site 4 were hard to determine using the same number of iterations as the other three test sites. Detailed sensitivity analyses were therefore performed for the initial permeability value k_o and stiffening parameter M (Figure 2.6b). In sites 1-3, both k_o and M were linearly independent. However, analysis at site 4 showed that the two parameters tended to be linearly dependent. Therefore, in order to uniquely determine k_o and M, the curve-fitting procedure required five additional iterations at site 4 than the required 5 for sites 1-3.

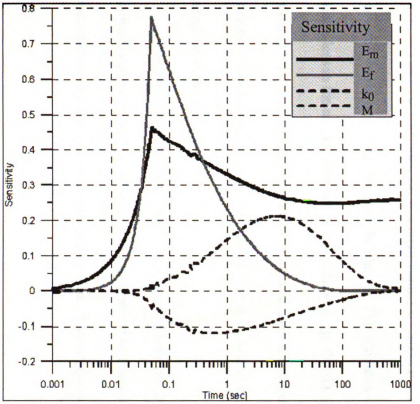

a

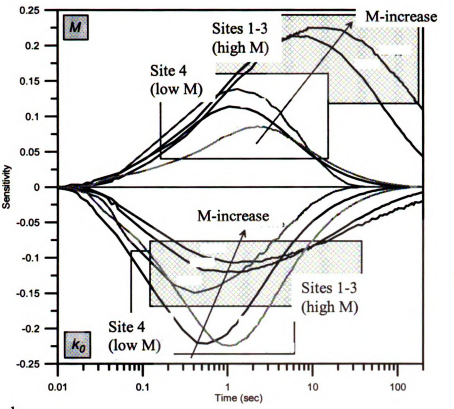

b

Figure 2.6 (a, b). a) Sensitivity graphs for the mechanical parameters were developed. b) The permeability and M were further analyzed by plateau location.

The analysis of indentation relaxation data from the left and right limbs at each site indicated no significant differences in any mechanical parameter or cartilage thickness. Therefore, these data were averaged for this study (Figure 2.7). The indentation tests did indicate, however, some differences in mechanical parameters between the medial and lateral facets, as well as between covered and uncovered areas of each facet. While in covered areas E_m was approximately 51% higher in the medial than lateral compartments ($p=0.05$), no differences were noted between facets in the uncovered areas ($p=0.77$). On the other hand, no significant difference in E_m was determined overall between the medial and lateral facets on the mature rabbit's tibial plateau ($p=0.33$). Overall across the plateau, E_m was approximately 48% higher in the uncovered areas than covered areas ($p=0.005$).

The fiber modulus, E_f, was significantly different medial to lateral, as well as in covered versus uncovered areas of the plateau. This modulus was, on average, nearly 4 times less in the medial than lateral compartments ($p<0.001$). While no difference in E_f existed between the uncovered lateral and medial compartments ($p=0.65$), there was nearly 7-fold decrease in E_f in the medial versus the lateral facets for meniscal covered areas ($p<0.001$).

Differences in permeability were also noted between the medial and lateral compartments, as well as between meniscal covered and uncovered areas. The initial permeability k_0 and factor M were each increased by approximately 90% in the medial

versus the lateral compartments ($p=0.005$). Both parameters were also higher by 95% ($p=0.003$) and 71% ($p<0.001$), respectively, in uncovered than covered areas.

The histological scores from the left and right limbs, as well as from the 3 readers were not significantly different, so the data were averaged for each specimen. On the other hand, some significant differences were evident between the medial and lateral facets (Figure 2.8).

More intense staining of the calcified cartilage was noted for medial versus lateral facets (Figure 2.9a,b). More disruptions of cartilage were also noted in the medial than the lateral compartments (Figure 2.9c,d). A trend ($p = 0.088$) was also indicated for there to be more histological-based fissures in sections from the medial than lateral compartments of the plateau (Figure 2.9e,f). On the other hand, no significant differences were recorded in the intensity of PG staining in the cartilage from the medial versus lateral facet.

Property		Medial				Lateral			
		Covered		Uncovered		Covered		Uncovered	
h	(mm)	**6.17E-01**	(1.39E-01)	**8.93E-01**	(1.07E-01)	**2.86E-01**	(7.25E-02)	**6.34E-01**	(1.04E-01)
E_m	(MPa)	**0.921**	(0.355)	**1.11**	(0.421)	**0.610**	(0.409)	**1.15**	(0.288)
E_f	(MPa)	**59.5**	(39.8)	**71.0**	(29.9)	**408.0**	(205.0)	**92.5**	(41.0)
k_0	(m^4/Ns)	**3.44E-14**	(2.40E-14)	**5.47E-14**	(1.76E-14)	**1.16E-14**	(1.17E-14)	**3.50E-14**	(2.82E-14)
M		**4.32E+01**	(1.67E+01)	**6.51E+01**	(9.93E+00)	**1.77E+01**	(6.81E+00)	**3.91E+01**	(1.09E+01)

Figure 2.7. Medial and lateral cartilage thickness and mechanical parameter results from the indentation relaxation test. The mean (bolded) and standard deviation (in parentheses) are given in this table.

	Medial		Lateral		P Value
CC Stain	1.77	(1.5-2.3)	1.27	(0.75-2.08)	0.001
Disruptions	2.23	(0.3-4.0)	1.4	(0.0-3.67)	0.043
Fissures	1.13	(0.25-1.67)	0.62	(0.0-1.67)	0.088
PG Staining	0.28	(0-.075)	0.2	(0-0.5)	NS

Figure 2.8. Histological score results from the medial and lateral facets. Results are given as the mean and range of data in parentheses.

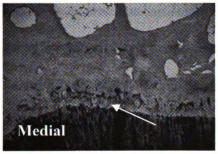

a

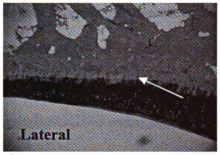

b

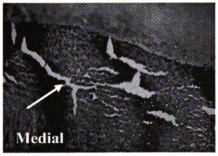

c

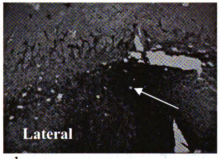

d

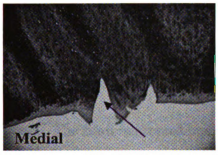

e

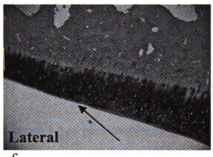

f

Figure 2.9 (a-f). Histological images of the articular cartilage and underlying bone show significant differences between the medial and lateral facets. The zone of calcified cartilage showed more intense staining for tissue proteoglycans medial (a) versus the lateral (b) facet, using a Safranin O-Fast Green protocol. The cartilage on the medial facet (c) showed more disruptions than the lateral facet (d). The tibial plateau showed more surface disruptions, including fissuring, on the medial (e) versus the lateral facet (f).

Overall, there were no significant differences between the thicknesses of calcified cartilage in medial (0.058 ± 0.014 mm) versus lateral (0.061 ± 0.012 mm) compartments, as well as between the medial (0.78 ± 0.07 mm) and lateral (0.80 ± 0.11 mm) subchondral plates. In contrast, there was a difference in the histological-based

measures of articular cartilage thickness between the medial (1.36 ± 0.19 mm) and lateral (0.93 ± 0.12 mm) compartments.

Statistically significant correlations were also documented between some of the histomorphological and mechanical parameters. For example, the length of surface fissures had a weak but significant negative correlation with fiber modulus (R^2 = -0.223, p = 0.035), and a weak but significant positive correlation with tissue permeability (R^2 = 0.24, p = 0.028). The fiber modulus also had a weak but significant negative correlation with articular cartilage thickness (R^2 = -0.264, p = 0.02). Finally, there was no indication of a statistical correlation between the intensity of cartilage PG stain and matrix modulus (R^2 = 0.00032, p = 0.9) or tissue permeability (R^2 = 0.043, p = 0.4) in the current study.

Discussion

The fibril reinforced biphasic model has previously been used to extract the mechanical properties of cartilage from experimental response data (Wilson et al., 2004). The model accurately fit the data from both the indentation and unconfined compression tests utilized in this study. In the current study the fibril reinforced biphasic model was used to closely fit the entire response curve from a single indentation relaxation experiment. The properties extracted from this model showed variation across the tibial plateau, as well as differences specifically in regions covered and uncovered by the meniscus. Surface fissuring and histologically identified matrix damage in articular cartilage documented in the medial compartment paralleled with reductions in fiber

modulus, and increases in permeability and tissue thickness in the medial versus lateral compartments of the plateau.

Numerous results from the current study could be compared with previous data by others, using either linear elastic or linear biphasic models of cartilage. These studies determined mechanical parameters from either the instantaneous or equilibrium response, which paralleled with the fiber or matrix modulus, respectively, in the current study using the fibril-reinforced biphasic model. Hoch et al. (1983), using the linear elastic cartilage model, as well as Roemhildt et al. (2006) using the linear biphasic model, both document no significant differences in the equilibrium modulus between medial and lateral facets of the rabbit tibial plateau for the central, uncovered regions. The current study also showed no significant differences in matrix modulus between the medial and lateral facets for the uncovered regions. However, the modulus was found to be greater on the medial versus lateral facet for regions covered by meniscus. These data compare to those of Rasanen and Messner (1996) using creep indentation tests in regions partially covered by the meniscus which document slightly stiffer cartilage in the medial than lateral facets. The current study also documented an over 40% higher matrix modulus in meniscal uncovered than covered regions of the plateau. Previous studies suggest that articular cartilage is stiffer, based on the equilibrium modulus, with a higher content of matrix proteoglycans in areas subjected to high versus low levels of stress (Kempson, 1979; Swann and Seedhom, 1986). The results of the current study on rabbits may then suggest larger joint pressures in uncovered than covered regions of the plateau, and especially in the medial compartment as indicated by the larger Em in the medial versus the lateral compartment. Studies on human specimens also show greater

pressures in the uncovered regions of the medial compartment, while high pressures are carried on both the uncovered and covered areas in the lateral compartment (Fukubayashi and Kurosawa, 1980; Walker and Erkman, 1975).

The equilibrium modulus correlates with the content of cartilage matrix PGs (Armstrong and Mow, 1982). More recently studies with the fibril reinforced biphasic model correlate PG stainability of cartilage with matrix modulus (Julkunen et al., 2007) However, in the current study, no statistical correlation was established between matrix modulus and PG stain intensity in the cartilage. A previous study suggests that the correlation between PG stain intensity and tissue stiffness may be related to the state of cartilage health (Camplejohn and Allard, 1988). In normal cartilage a direct correlation could be established between these tissue properties, but not in osteoarthritic cartilage. This may be due to the reduction of anions in the matrix and therefore, a reduction of possible binding sites for the safranin-O stain (Camplejohn and Allard, 1988). The lack of a correlation in the current study may then suggest the tissue may be in a diseased state of health.

The instantaneous response of the cartilage was also fit with the fibril-reinforced biphasic model in this study. The sensitivity studies suggested that the peak load during these experiments was most sensitive to fiber modulus, a mechanical parameter that likely reflects the mechanical characteristics of the network of collagen (Korhonen et al., 2003; Julkunen et al., 2007). In a previous study on central areas of the rabbit tibial plateau a slightly lower instantaneous modulus using the linear elastic model was documented in the medial than lateral facets (Wei et al., 1998). The result compares well with the fiber modulus data of the current study. Additionally, the current study

established a statistically significant negative correlation between fiber modulus and the length of surface fissures. Surface fissures and tissue swelling are early characteristics of osteoarthritis that have been related to the early degradation of the collagen network (Bank et al., 2000; Pelletier et al., 1983; Verzijl et al., 2002). The correlation documented between increases in tissue permeability with fissure length helps explain differences documented in the medial versus lateral compartments and meniscal uncovered versus covered areas of the plateau, and the results compare with early studies on the development of osteoarthritis using the knee ligament transection model (Setton et al., 1994).

We also documented an increase in the PG stain intensity in the zone of calcified cartilage in the medial versus lateral facet. This histological feature may suggest that the zone of calcified cartilage in the medial facet was in more of an active state of remodeling than the lateral facet (Oegema and Thompson, 1992). This histological feature also paralleled with more matrix disruptions and surface fissuring of cartilage on the medial than lateral facets in this animal model. It is currently unclear whether these changes in tissue quality result from more or less load being carried by the medial versus lateral facets. In human (Kemp et al., 2008) and animal studies (Rasanen and Messner,1996) the excessive levels of tissue degradation noted in medial versus lateral facets are suggested to be the result of more loading on the medial facet. On the other hand, studies suggest the degenerative state of this tissue in medial versus lateral facets may be due to a lower level of load in the medial compartment (Chang et al., 1997). This suggestion may well support the observation made recently in rabbit gait studies that show a slightly larger joint load being carried by the lateral compartment during a hop

(Gushue et al., 2005). On the other hand, the current study indicates a larger matrix modulus in the medial versus lateral compartments, suggestive of possibly greater levels of loading medial than lateral. Thus, additional studies are needed to clarify these apparent contradictory results.

In terms of tissue permeability and fibril modulus in covered areas of the plateau, the current study showed larger medial to lateral differences than most literature. This could be due to relatively more intense loading on the medial than lateral facets, or vice versa, in the exercised model used in the current study. None of the previous studies have used a regularly exercised model, nor have results been gathered on the larger, Flemish Giant rabbit. Previous studies on other animal models have shown that while moderate intensities of regular exercise have a positive effect on joint cartilage (Jurvelin et al., 1990; Newton et al., 1997), more intense exercise or unloading can have a negative effect on the joint cartilage (Helminen et al., 1992). While our laboratory has not performed gait analysis on our model or quantified the intensity of the exercise protocol, these rabbits did subjectively appear exhausted after each daily session of treadmill activity, suggesting a rather intense level of exercise for the animal.

Future studies will be needed to better define potential relationships between alterations in the joint loading and changes in tissue properties across the tibial plateau in the human and various animal models. The current study helps support the notion that a more complex fibril-reinforced, biphasic model of the cartilage in such studies may lead to more consistent mechanical results that correlate with histomorphological changes noted in articular cartilage.

Acknowledgements

This study was supported by the Centers for Disease Control and Prevention, the National Center for Injury Prevention and Control (CE000623). Its contents are the responsibility of the authors and do not necessarily represent the official views of the Centers for Disease Control and Prevention. The authors thank Jane Walsh (JW) and Derek Handzo (DH) for their contributions on the histology aspects of the study, as well as and Jean Atkinson (JA) for exercising and care of the animals and Eric Meyer for mechanical testing and histological scoring.

References

Armstrong, C.G. and Mow, V.C. (1982) Variations in the intrinsic mechanical properties of human articular cartilage with age, degeneration, and water content. *Journal of Bone and Joint Surgery* Am. **64**, 88-94.

Athanasio, K.A., Rosenwasser, M.P., Buckwalter, J.A., Malinin, T.I., and Mow, V.C. (1991) Interspecies comparison of in situ intrinsic mechanical properties of distal femoral cartilage. *Journal of Orthopaedic Research* **9**,.330-340.

Bank, R.A., Soudry, M., Maroudas, A., Mizrahi, J., and TeKoppele, J.M. (2000) The increased swelling and instantaneous deformation of osteoarthritic cartilage is highly correlated with collagen degradation. *Arthritis and Rheumatism* **43**, 2202-2210.

Beck, J. and Arnold, K. (1977). *Parameter Estimation in Engineering and Science*, New York: John Wiley and sons.

Camplejohn, K.L. and Allard, S.A. (1988) Limitations of safranin 'O' staining in proteoglycan-depleted cartilage demonstrated with monoclonal antibodies. *Histochemistry* **89**, 185-188.

Chang, D.G., Iverson, E.P., Schinagl, R.M., Sonoda, M., Amiel, D.,Coutts, R.D., and Sah, R.L., (1997) Quantitation and localization of cartilage degeneration following induction of osteoarthritis in the rabbit knee. *Osteoarthritis and Cartilage* **5**, 357-372.

Colombo, C., Butler, M., O'Byrne, E., Hickman, L., Swartzendruber, D., Selwyn, M., and Steinetz, B. (1983) A new model of osteoarthritis in rabbits. I. Development of knee joint pathology following lateral meniscectomy and section of fibular collateral and sesamoid ligaments. *Arthritis Rheumatology* **26**, 875-886.

Ewers, B.J., Weaver, B.T., Sevensma, E.T., and Haut, R.C. (2002) Chronic changes in rabbit retro-patellar cartilage and subchondral bone after blunt impact loading of the patellofemoral joint. *Journal of Orthopaedic Research* **20**, 545-550.

Fukubayashi, T. and Kurosawa, H. (1980) 'The contact area and pressure distribution pattern of the knee. *Acta Orthopaedica Scandinavica* **51**, 871-879.

Gushue, D.L., Houck, J., and Lerner, A.L. (2005) Rabbit knee joint biomechanics: motion analysis and modeling of forces during hopping. *Journal of Orthopaedic Research* **23**, 735-742.

Haut, R.C., Ide, T.M., and DeCamp, C.E. (1995) Mechanical responses of the rabbit petello-femoral joint to blunt impact. *Journal of Biomechanical Engineering* **117**, 402-408.

Hayes, W.C., Keer, I.M., Herrmann, G., and Mockros, I.E. (1972) A mathematical analysis for indentation tests of articular cartilage. *Journal of Biomechanics* **5**, .541-551.

Helminen, H., Kiviranta, I., Saamanen, A., Jurvelin, J., Arokoski,J., Oettmeier, R. (1992) Effect of motion and load on articular cartilage in animal models. *Articular Cartilage and Osteoarthritis* **35**, 501–510.

Hoch, D., Grodzinsky, A., Koob, T., Albert, M., and Eyre, D. (1983) Early changes in material properties of rabbit articular cartilage after meniscectomy. *Journal of Orthopaedic Research* **1**, 4-12.

Jin, H. and Lewis, J.L. (2004) Determination of Poisson's ratio of articular cartilage by indentation using different-sized indenters. *Journal of Biomechanical Engineering* **126**, 138-145.

Julkunen, P., Kiviranta, P., Wilson, W., Jurvelin, J.S., and Korhonen, R.K. (2007) Characterization of articular cartilage by combining microscopic analysis with a fibril-reinforced finite-element model. *Journal of Biomechanics* **40**, 1862-1870.

Jurvelin, J., Kiviranta, I., Saamanen, A.M., Tammi, M., and Helminen, H.J. (1990) Indentation stiffness of young canine knee articular cartilage-influence of strenuous joint loading. *Journal of Biomechanics* **23**, 1239-1246.

Kemp, G., Crossley, K.M., Wrigley, T.V., and Metcalf, B.R. (2008) Reducing joint loading in medial knee osteoarthritis: shoes and canes. *Arthritis and Rheumatism* **59**, 609-614.

Kempson, G.E. (1979) Mechanical properties of articular cartilage. *In*: Freeman, M.A.R. (ed.), *Adult Articular*, 333–414 London: Pitman Medical.

Kiviranta, P., Rieppo, R.K., Julunen, P., Toyras, J., and Jurvelin, J.S. (2006) Collagen network primarily controls Poisson's ratio of bovine articular cartilage in compression. *Journal of Orthopaedic Research* **24**, 690-699.

Korhonen, R.K., Laasanen, M.S., Toyras, J., Lappalainen, R., Helminen, H.J., and Jurvelin, J.S. (2003) Fibril reinforced poroelastic model predicts specifically mechanical behavior of normal, proteoglycan depleted and collagen degraded articular cartilage. *Journal of Biomechanics* **36**, 1373-1379.

Li, L.P., Buschmann, M., and Shirazi-Adl, A. (2000) A fibril reinforced nonhomogeneous poroelastic model for articular cartilage: Inhomogeneous response in unconfined compression. *Journal of Biomechanics* **33**, 1533-1541.

Li, L.P., Soulhat, J., Buschmann, M.D., and Shirazi-Adl, A. (1999) Nonlinear analysis of cartilage in unconfined ramp compression using a fibril reinforced poroelastic model. *Clinical Biomechanics* **14**, 673-682.

Lindstrom, P., and Wedin, P.A. (1993) *A method of gauss-newton type for nonlinear least-squares problems with nonlinear constraints*. Technical Report UMINF-133.87, Inst. Of Information Processing, University of Umea, Umea, Sweden.

Lipshitz, H., Etheridge, R., and Glimcher, M.J. (1975) In vitro wear of articular cartilage. *Journal of Bone and Joint Surgery* **57**, 527-537.

Mansour, J.M., Wentorf, F.A., and Degoede, K.M. (1998) In vivo kinematics of the rabbit knee in unstable models of osteoarthritis. *Annals of Biomedical Engineering* **26**, 353-360.

Mazieres, B., Blanckaert, A., and Thiechart, M. (1987) Experimental post-contusive osteoarthritis of the knee: quantitative microscope study of the patella and the femoral condyles', *Journal of Rheumatology* **14**, 119-121.

Mow, V.C., Kuei, S.C., Lai, W.M., and Armstrong, C.G. (1980) Biphasic creep and stress relaxation of articular cartilage in compression: Theory and experiments. *Journal of Biomechanical Engineering* **102**, 73-84.

Newton, P.M., Mow, W.C., Gardner, T.R., Buckwalter, J.A., and Albright, J.P. (1997) The effect of lifelong exercise on canine articular cartilage. *American Journal of Sports Medicine* **25**, 282–287.

Oegema, T.R., Carpenter, R.J., Hofmeister, F., and Thompson, R.C. Jr. (1997) The interaction of the zone of calcified cartilage and subchondral bone in osteoarthritis. *Microscopy Research and Technique* **37**, 324-332.

Oyen-Tiesma, M., Atkinson, J., and Haut, R.C. (1998) A method for promoting regular exercise in rabbits involved in orthopedics research. *Contemporary Topics in Laboratory Animal Science* **37**, 77-80.

Parsons, J.R. and Black, J. (1977) The viscoelastic shear behavior of normal rabbit articular cartilage. *Journal of Biomechanics* **10**, 21-29.

Pelletier, J.P., Martel-Palletier, J., Altman, R.D., Ghandur/Mnaymneh, L., Hower, D.S., and Woessner, J.F., (1983) Collagenolytic activityand collagen matrix breakdown of the articular cartilage in de Pond-Nuki dog model of osteoarthritis. *Arthritis and Rheumatism* **26**, 866-874.

Rasanen, T. and Messner, K. (1996) Regional variations of indentation stiffness and thickness of normal rabbit knee articular cartilage. *Journal of Biomedical Materials Research* **31**, 519-524.

Roemhildt, M.L., Coughlin, K.M., Peura, G.D., Fleming, B.C., and Beynnon, B.D. (2006) Material properties of articular cartilage in the rabbit tibial plateau. *Journal of Biomechanics* **39**, 2331-2337.

Sah, R.L., Yang, A.S., Chen, A.C., Hant, J.J., Halili, R.B., Yoshioka, M., Amiel, D., and Coutts, R.D. (1997) Physical properties of rabbit articular cartilage after transition of the anterior cruiate ligament. *Journal of Orthopedic Research* **15**, 197-203.

Setton, L.A., Mow, V.C., Muller, F.J., Pita, J.C., and Howell, D.S. (1994) Mechanical properties of canine articular cartilage are significantly altered following transection of the anterior cruciate ligament. *Journal of Orthopaedic Research* **12**, 451-463.

Swann, A.C. and Seedhom, B.B. (1986) The relationship between the stiffness of normal articular cartilage and predominant acting stress levels. *Publ. Univ. Kuopio Med. Orig. Rep* **6**, C3.

van der Voet, A. (1997) A comparison of finite element codes for the solution of biphasic poroelastic problems. *Proceedings of the Institute of Mechanical Engineering* **211**, 209-211.

Verzijl, N., DeGroot, J., Zaken, C.B., Braun-Benjamin, O., Maroudas, A., Bank, R.A., Mizrahi, J., Schalkwaijk, C.G., Thorpe, S.R., Baynes, J.W., Bijlsma, J.W.J., Lafeber, F.P.J.G., and TeKoppele, J.M. (2002) Crosslinking by advanced glycation end products increases the stiffness of the collagen network in human articular cartilage. *Arthritis and Rheumatism* **46**, 114-123.

Vignon, E., Bejui, J., Mathieu, P., Hartmann, J.D., Ville, G., Evreux, J.C., and Descotes, J. (1987) Histological cartilage changes in a rabbit model of osteoarthritis. *Journal of Rheumatology* **14**, 104-106.

Walker, P.S. and Erkman, M.J. (1975) The role of the menisci in force transmission across the knee. *Clinical Orthopaedics* **106**, 184-192.

Weaver, B.T. and Haut, R.C. (2005) Enforced Exercise after blunt trauma significantly affects biomechanical and histological changes in rabbit retro-patellar cartilage. *Journal of Biomechanics* **38**, 1177-1183.

Wei, X., Rasanen, T., and Messner, K. (1998) Maturation-related compressive properties of rabbit knee articular cartilage and volume fraction of subchondral tissue. *Osteoarthritis and Cartilage* **6**, 400-409.

Wilson, W., van Donkelaar, C.C., van Rietbergen, B., and Huiskes, R. (2005) A fibril-reinforced poroviscoelastic swelling model for articular cartilage. *Journal of Biomechanics* **38**, 1195-1204.

Wilson, W., van Donkelaar, C.C., van Rietbergen, B., Ito, K., and Huiskes, R. (2004) Stress in the local collagen network of articular cartilage: a poroviscoelastic fibril-reinforced finite element study. *Journal of Biomechanics* **37**, 357-366.

Zhang M., Zheng, Y.P., and Mak, A.F. (1997) Estimating the effective young's modulus of soft tissues from indentation tests-nonlinear finite element analysis of effects of friction and large deformation. *Medical Engineering and Physics* **19**, 512-517.

Chapter 3

High levels of glucosamine-chondroitin sulfate can alter articular cartilage stiffness and up-regulate proteoglycan content of bovine chondral explants following unconfined compression injury

Abstract

Traumatic injury to articular cartilage results in chondrocyte loss, collagen damage and decreased PG content and has been found to be load level and strain dependent. Therapeutic agents, such as glcN-CS, have been shown to increase the PG content of cartilage pre-trauma and; therefore, increase the compressive stiffness. A hypothesis of the current study was that significantly more damage will occur following a higher level of trauma documented by lower mechanical properties and a decrease in PG content of the tissue. A second hypothesis of the study was that treatment with glcN-CS in the post-trauma period will up regulate the PG content of the injured explants and therefore, help maintain its pre-trauma mechanical stiffness. Bovine chondral explants were loaded with 10 MPa or 25 MPa of unconfined compression with and without glcN-CS treatment. Mechanical properties were extracted at 7, 14, and 21 days and following 21 days PG content was analyzed. A 25 MPa unconfined compression significantly decreased the mechanical properties of the cartilage compared to tissues that were loaded with 10 MPa of unconfined compression. Treatment with glcN-CS significantly increased the PG content and matrix modulus compared to untreated samples following both 10 and 25 MPa of unconfined compression. The results of this study confirm the ability of glcN-CS to increase the PG content in the tissue following traumatic injury, increasing the matrix stiffness. Future studies should focus on the effects of glcN-CS treatment in the long term as it may provide better outcomes for the ACL repaired patient.

Introduction

Traumatic injury to articular cartilage during participation in sports, recreation and exercise (SRE) frequently leads to the development of a chronic joint disease, osteoarthritis (OA). Two specific types of injuries are associated with subsequent knee OA: cruciate ligament damage and meniscal tears (Felson et al., 2004). Evidence in the clinical literature suggests that 50-70% of patients with complete anterior cruciate ligament (ACL) rupture and associated injuries develop radiological signs of OA within 15-20 years (Gillquist and Messner, 1999). And, surgical reconstruction of the torn ACL is not effective in mitigating the incidence of joint OA, as a significant portion of these patients develop clinical symptoms of OA 5-10 years post-injury (Daniel et al., 1994). Arthroscopic surgeries have documented softening and fissuring of cartilage overlying so call "geographic" bone bruises in the ACL injured patient, and biopsy specimens from these patients reveal degeneration and death of chondrocytes in this area (Fang et al., 2001; Johnson et al., 1998). This damage to articular cartilage is thought to be caused by excessive compressive forces generated in the joint during the acute injury and has been hypothesized to form the basis for the subsequent development of OA (Fang et al., 2001).

In vitro studies have documented significant changes in the articular cartilage following traumatic loading, such as an increase in tissue wet weight (Loening et al., 2000, Huser and Davies, 2006), damage to the collagen network (Torzilli et al., 1999) and decreased chondrocyte viability (Huser and Davies, 2006; Loening et al., 2000; Kurz et al., 2001) and proteoglycan (PG) content (Huser and Davies, 2006; Patwari et al., 2000). The level of damage is dependent on compressive loading levels and strain rates (Torzilli et al., 1999). Specifically, traumatic loading to the cartilage explants increases

the percentage of dead cells with increasing loading levels (6-20 MPa), with significantly more apoptotic cells documented above 10 MPa (Loening et al., 2000). Additionally, a study by Kurz et al. (2001) documents an increase in cell death with increasing strain rate ($0.01\text{-}1s^{-1}$) of compression and the remaining viable cells have a significant decrease in biosynthetic activity at 0.1 s^{-1} and 1 s^{-1}. Chondrocyte damage leaves the cartilage with few metabolically active cells to repair the degraded matrix (Loening et al., 2000). One specific function of chondrocytes is the synthesis of proteoglycans (PGs) and loss of chondrocytes has been correlated with a loss of tissue PGs (Huser and Davies, 2006; Simon et al., 1976). Previous studies have documented the loss of PG in cartilage explants following compressive loading (Huser and Davies, 2006; Patwari et al., 2000) and this loss of PG has been correlated with a decrease in compressive stiffness (Patwari et al. 2000). These degenerative changes may be due to an increase in degenerative enzymes (Lin et al., 2004). Cartilage softening has been documented in patients following traumatic injury and has been associated with the development of OA. Since proteoglycans are responsible for the resistance to stress and strain and loss of PG is correlated with cartilage softening (Patwari et al., 2000), prevention of PG loss may help in retaining the cartilage stiffness and resistance to compressive loading after injury.

Therapeutic agents, such as glucosamine (glcN) and chondroitin sulfate (CS), can increase the PG content of cartilage and therefore increase matrix properties like compressive stiffness. Clinical trials have shown that daily oral supplements of glcN for 3 years can slow the progression of joint disease, by mitigating joint space narrowing (Richy et al. 2003), although no evaluation of the mechanical or biological properties were conducted in this particular study. Tiraloche et al. (2005), in another study,

document an increase in histological PG stain in ACL transected rabbits treated for 8 weeks with daily supplements of oral glcN compared to untreated animals. Additionally, bathing chondral explants in a supplement of glcN and CS up-regulates the synthesis of tissue PG's (Lippiello, 2003). Treatment with glcN-CS has been documented to decrease the effects of degradative enzymes (Dodge and Jimenez, 2003). The objective of the current study was to document the mechanical properties and PG content of chondral explants following unconfined compression, with and without glcN-CS treatment post-trauma. Two levels of unconfined compression (10 MPa and 25 MPa) were used to evaluate varying levels of trauma as previous studies have documented degeneration effects to be load dependent. A hypothesis of the current study was that significantly more damage will occur following a higher level of trauma documented by lower mechanical properties and a decrease in PG content of the tissue. A second hypothesis of the study was that treatment with glcN-CS in the post-trauma period will up regulate the PG content of the injured explants and therefore, help maintain its pre-trauma mechanical stiffness. This may help maintain post-trauma tissue homeostasis and help preserve the functionality of traumatized joint cartilage.

Method

Dissection and tissue culture

Skeletally mature bovine forelegs (18-24 months of age) were obtained from a local abattoir within 2 hours of slaughter. The legs were rinsed with water and skinned prior to exposing the metacarpal joint. A 6 mm diameter biopsy punch (Miltex Instrument Company, Bethpage, NY) was used to make chondral explants from the lower metacarpal

surface of each limb under a laminar flow hood. Explants were separated from the underlying bone with a scalpel. All specimens were washed three times in Dulbecco's Modified Eagle Media: F12 (DMEM: F12) (Gibco, USA, #12500-039) supplemented with additional amino acids and antibiotics (penicillin 100 U/ml, streptomycin 1 μg/ml, amphotericin B 0.25 μg/ml). The osmolarity of the media was 300mosM (Osmete 2, Precision Systems), and the pH was 7.4 as this has previously been shown to result in physiological and metabolic stability of the explants (Phillips and Haut 2004; Baars et al. 2006; Wei et al. 2008; Wei and Haut 2009). The explants were randomly assigned to two impact groups: 10 MPa and 25 MPa. Each of these groups was further divided into two sub groups, with and without glcN-CS: '10 MPa with glcN-CS' (n=8), '10 MPa without glcN-CS' (n=12), '25 MPa with glcN-CS' (n=8), and '25 MPa without glcN-CS' (n=12). The explants were then placed in a 24-well plate in media supplemented with 10% fetal bovine serum (Gibco, USA, #16000). The treated samples were bathed in supplemented media with glucosamine and chondroitin sulfate supplement (glcN-CS) (500 μg/mL glcN (FCHG49®) and 250 μg/mL CS (TRH122®)). GlcN-CS concentrations were chosen based on previous studies (Rundell et al., 2005; Wei et al., 2008) to maximize treatment effects. The media was replaced every 2 days during the study.

Indentation testing of explants

All samples were allowed to equilibrate for 24 hours after harvesting inside of a humidity-controlled incubator (37°C, 5% CO_2, 95% humidity). Prior to impact, each explant was subjected to mechanical testing using an indentation stress relaxation test to extract the mechanical properties of the explants prior to compressive loading. These data

served as baseline mechanical property data and were used to normalize the data following compressive loading. Indentation tests on each explant were also performed 7, 14, and 21 days following impact. Prior to mechanical testing, the cartilage explant thickness was measured twice at perpendicular orientations across the center of the explant using a digital vernier caliper (Mitutoyo Corp.: Absolute Digimatic, Model No. CD-6" CS) with a resolution of 0.01 mm (Steinmeyer et al., 1997 and 1999). The two thickness values were then averaged. The explants were placed on a flat level surface so that the face of the explant was perpendicular to the indenter tip (Figure 3.1B). A magnet with a 4.3 mm diameter hole was placed on top of the explant to secure the edges from curling (Figure 3.1C). The explant and fixture were then submerged into a room-temperature phosphate buffered saline solution (PBS with pH 7.2) (Figure 3.1A). A 2.39 mm diameter spherical, non-porous probe was lowered into the cartilage until a preload of 0.05 N was attained and held for 60 s (Figure 3.1D). The indenter was then pressed into the cartilage 25% of the thickness in 2 s and maintained for 600 s while resistive loads of relaxation were recorded (Data Instruments, Acton, MA: model JP-25, 25 lb capacity), amplified and sampled at 1,000 Hz for the first second, and 20 Hz thereafter. The stress relaxation curves were fitted to a fibril-reinforced biphasic model (Soulhat et al., 1999; Golenberg et al., 2009) with an assumed Poisson's ratio of 0.25. The matrix modulus (E_m), fiber modulus (E_f) and tissue permeability (k_0) were evaluated in the computational model using a custom-written Gauss-Newton constrained nonlinear least square minimization procedure.

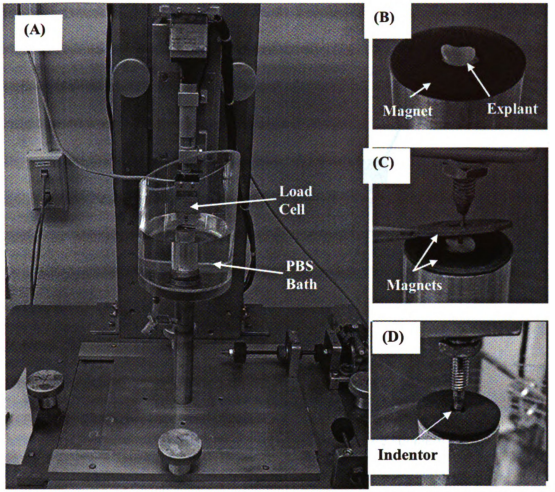

Figure 3.1. Explant indentation test system and fixture (A). The explants were placed in a hole in the bottom magnet on a flat steel surface (B). A top magnet was lowered over the top of the explant to hold down the edges (C). The spherical indentor tip was lowered to a preload of 0.05 N (D).

Unconfined compression

Following a 5 N preload the explants were taken to either 282 N (~10 MPa) or 707 N (~25 MPa) in unconfined compression between two polished stainless steel plates (Figure 3.2). A 0.5 Hz (1 s time to peak) haversine loading protocol was programmed in a servo-controlled hydraulic testing machine (Instron, model 1331, retrofitted with 8500 plus electronics, Canton, MA). Immediately after compressive loading, all explants were placed in the incubator for the duration of the study.

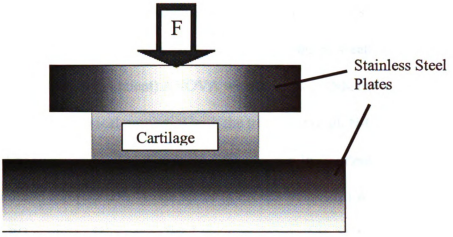

Figure 3.2. Cartilage explants were loaded (10 MPa or 25 MPa) in unconfined compression between two polished stainless steel plates.

Determination of Proteoglycan (PG) Content

After 21 days, the sample wet weights were recorded. Approximately, 4.5 mg Chondroitin Sulfate A sodium salt from bovine trachea (Sigma-ALDRICH GmbH Steinheim, Germany) was measured out and used to generate standard curves (Steinmeyer et al. 1999). The samples and the standards were digested overnight at 60 °C in a papain solution: PBS, EDTA, cysteine and papain. Papain digested cartilage explants and the standards were dimethyl-methylene blue (DMB) assayed for sulfated PGs by the reaction with 1, 9-DMB dye solution in polystyrene 96 well plates and quantitated with spectrophotometry at wavelength 530 nm using a Bio Tek microplate reader. PG content was normalized to cartilage wet weights.

Statistical Analysis

Mechanical property data obtained from post-impact explants were normalized using the pre-impact values to document change in each property. Statistical analysis was used to evaluate differences in mechanical and biochemical properties. A two-factor (day,

load group) ANOVA with a posthoc Student-Newman-Keuls (SNK) test was used to determine differences in mechanical properties between the treatment groups. A two-factor (day, glcN-CS treatment) ANOVA with a posthoc SNK test was used to determine differences in mechanical properties with the treatment of glcN-CS. A one factor (load group) ANOVA was used to document differences in PG content between the two levels of unconfined compression. A one factor (glcN-CS treatment) ANOVA was used to analyze PG content of the unconfined compression groups. Statistical significance was indicated at $p<0.05$.

Results

Unconfined Compression

Both the 10 MPa and 25 MPa of unconfined compression resulted in surface fissures seen following staining of the articular surface with India ink. Gross assessment revealed more surface lesions in the samples loaded to 25 MPa. These samples also appeared elliptical in shape.

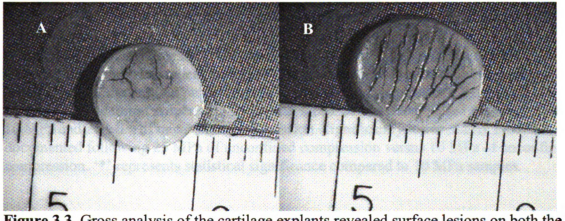

Figure 3.3. Gross analysis of the cartilage explants revealed surface lesions on both the 10 MPa (A) and 25 MPa (B) samples with more fissures on the 25 MPa samples. These samples also appeared elliptical in shape.

Indentation Testing

The E_m decreased approximately 20% and 40% at 10 MPa and 25 MPa of unconfined compression, respectively. No decrease in E_m was noted over 21 days. A significant decrease in E_m was found in the 25 MPa samples compared to the 10 MPa samples at 7 ($p<0.001$), 14 ($p=0.004$) and 21 ($p=0.004$) days following unconfined compression (Figure 3.4).

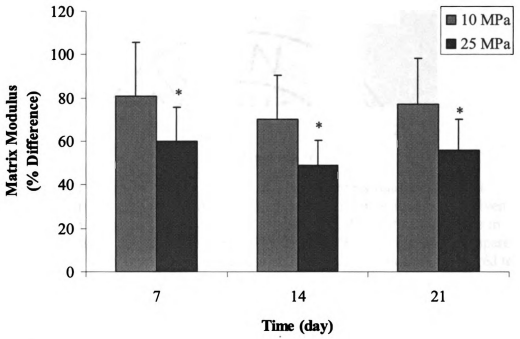

Figure 3.4. The matrix modulus was determined from the stress-relaxation curves documented during each indentation test. The matrix modulus presented here is given as a percentage of the original property prior to unconfined compression. A decrease, compared to the initial property, in the matrix modulus was documented following both 10 MPa and 25 MPa of unconfined compression. Significantly lower matrix modulus was documented following 25 MPa of unconfined compression versus 10 MPa of unconfined compression. '*' represents statistical significance compared to 10 MPa samples.

The permeability increased by approximately 140% and 250% following 10 MPa and 25 MPa of unconfined compression, respectively. No changes in permeability were documented between 7, 14, and 21 days. A statistical increase in the permeability was

noted in the 25 MPa versus 10 MPa samples at 7 ($p=0.007$), 14 ($p=0.005$), and 21 ($p<0.001$) days (Figure 3.5).

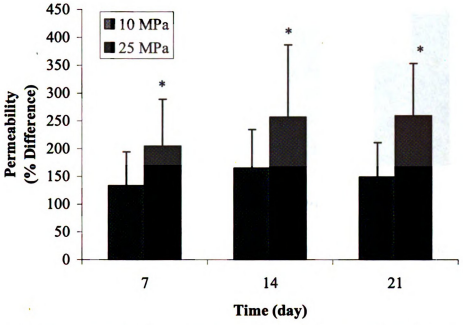

Figure 3.5. The permeability was determined from the stress-relaxation curves documented during each indentation test. The permeability presented here is given as a percentage of the original property prior to compression. A significant increase in permeability was documented following 25 MPa unconfined compression compared to 10 MPa unconfined compression. '*' represents statistical significance compared to 10 MPa samples.

A 150% increase in the E_f was documented in the 25 MPa samples. No such increase was noted in samples compressed to 10 MPa. This increase in E_f was significantly greater at 25 MPa compared to the 10 MPa at 7 ($p=0.042$) and 21 ($p=0.016$) days with a statistical trend for an increase at 14 days ($p=0.096$) (Figure 3.6). No change in E_f was documented between 7, 14, and 21 days.

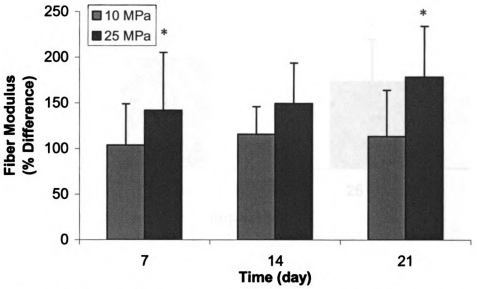

Figure 3.6. The fiber modulus was determined from the stress-relaxation curves documented during each indentation test. The fiber presented here is given as a percentage of the original property prior to compression. An increase in the fiber modulus was documented following 25 MPa unconfined compression compared to original property and this increase was significantly higher than samples following 10 MPa of unconfined compression '*' represents statistical significance compared to the 10 MPa samples.

Biochemical assays revealed a decrease in matrix PG content in the 25 MPa samples compared to the 10 MPa, however, this decrease did not rise to a level of statistical significance (Figure 3.7).

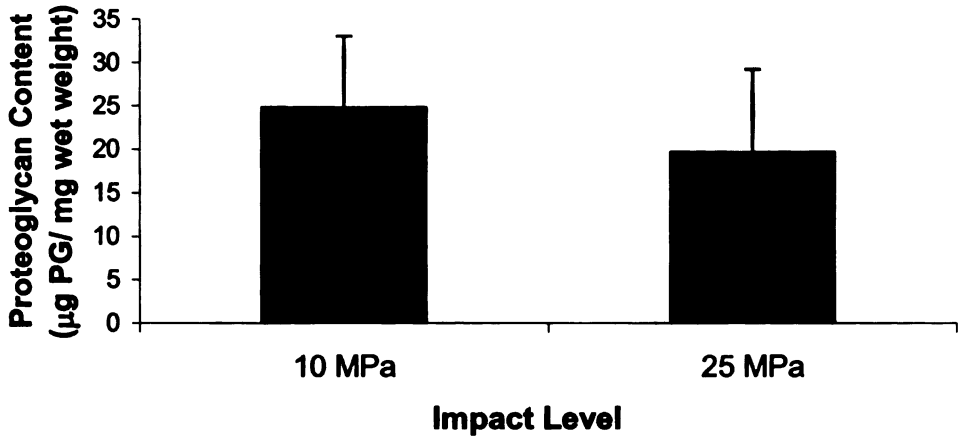

Figure 3.7. Proteoglycan content in samples was determined using DMB assay. Results are shown here as µg PG per mg wet weight. No statistical difference was documented in the PG content between 10 MPa and 25 MPa of unconfined compression.

Treatment with glcN-CS

An increase in E_m was documented in the '10 MPa with glcN-CS' versus '10MPa without glcN-CS' at day 7 ($p=0.033$) and 14 ($p=0.048$) days, with statistical trend for an increase at day 21 ($p=0.06$) (Figure 3.8). Similarly, an increase in the matrix modulus was documented between the samples treated with glcN-CS versus the untreated samples at 7, 14 ($p=0.1$), and 21 days following 25 MPa of unconfined compression, however, this difference did not rise to a level of statistical significance (Figure 3.9). No significant differences were documented between treated and untreated samples in the fiber modulus or permeability in either unconfined compression group.

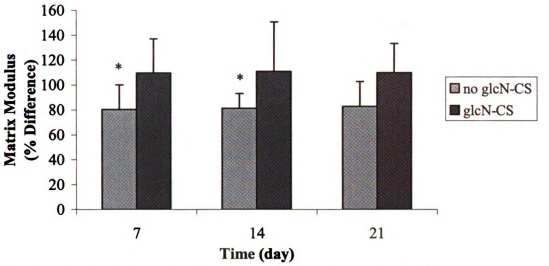

Figure 3.8. The matrix modulus of the 10 MPa samples with and without glcN-CS was determined from stress-relaxation curves. A significant increase in the matrix modulus was documented following treatment with glcN-CS compared to untreated samples. '*' denotes statistical significance compared to samples treated with glcN-CS.

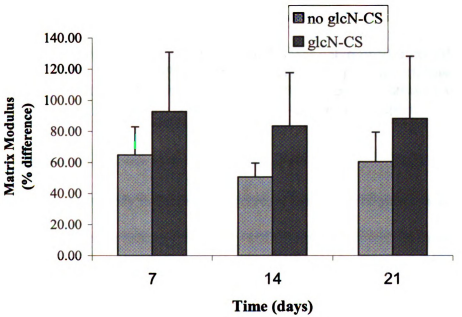

Figure 3.9. The matrix modulus of the 25 MPa samples with and without glcN-CS was determined from stress-relaxation curves. An increase in the matrix modulus was documented following treatment with glcN-CS compared to untreated samples; however, statistical significance was not reached.

A significant increase in PG content was documented in the treated samples compared to the untreated samples for both 10 MPa ($p<0.001$) and 25 MPa ($p=0.023$) of unconfined compression (Figure 3.10).

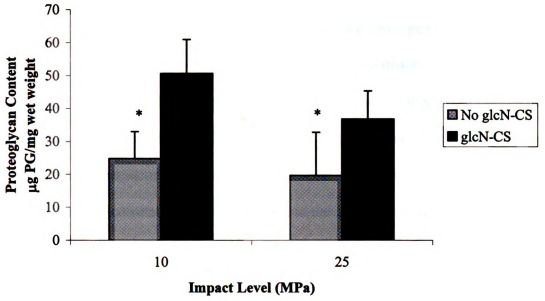

Figure 3.10. Proteoglycan content in all samples was determined using DMB assay. Results are shown here as µg PG per mg wet weight. A significant increase in PG content was documented in samples treated with glcN-CS compared to untreated samples. '*' denotes statistical significance compared to glcN-CS treated samples.

Discussion

The current study documented a decrease in the matrix modulus and PG content with an increase in the tissue permeability and fiber modulus with an increasing level of unconfined compression. These results correlate with previous studies that documented decreased cartilage stiffness and increased fluid parameters following traumatic injury with a loss of PG in the tissue (Kurz et al., 2001; Loening et al., 2000). Interestingly, an increase in the fiber modulus was documented following a 25 MPa of unconfined compression, with no change in modulus following 10 MPa of unconfined compression.

Torzilli et al. (1999) documents that loading at or above a critical threshold of 15-20 MPa causes permanent damage to the collagen network and an increase in the tissue water content. In the current study, a change in the cartilage shape and an increase in surface disruptions were documented following 25 MPa of unconfined compression. Previous studies have documented that following an impact load, the cartilage becomes flattened fissured and elliptical in shape and that the alignment of these distortions reflect the orientation of the collagen fibers (Jeffrey et al., 1995). In the current study, a change in shape and increased fissuring were found following 25 MPa of unconfined compression and, therefore, reflect damage to the collagen network. Additionally, previous studies have documented a correlation between damage to the collagen network and tissue swelling (Bank et al., 2000; Khalsa and Eisenberg, 1997), as the collagen network is known to resist the swelling of cartilage. Therefore I suggest that, following traumatic injury to the collagen network, swelling pressures increase and therefore, the remaining intact collagen fibers bear more tension. The increase in fiber modulus from the current study may reflect this increase in tension in the intact collagen fibers and the increase in swelling pressure following the 25 MPa of unconfined compression. However, cartilage swelling and content of collagen were not measured in the current study.

The current study also showed an increase in tissue PG content with glcN-CS treatment that was reflected by an increase in tissue E_m. These results compare with previous findings by our laboratory documenting an increase in PG content and matrix stiffness following treatment of bovine chondral explants with glcN-CS (Wei and Haut, 2008). Interestingly, Tiraloche et al. (2005) also document an increase in the PG content

in the rabbit articular cartilage following ACL transection with an oral treatment of glcN-CS.

Previous studies suggest a possible explanation for the decrease in mechanical properties is the increase in degenerative enzymes. Injurious compression has been shown to increase MMP-3 resulting in the degradation effects in the matrix parameters (Lin et al., 2004). A previous study suggests that treatment with glcN-CS may inhibit the effects of MMP-3s (Dodge and Jimenez, 2003). The current study did not documente MMP-3 concentrations. Future studies should focus on the effects of these inhibiting these enzymes following traumatic injury with glcN-CS treatment post-trauma.

The current study suggests that post-trauma treatment with glcN-CS effectively increased matrix stiffness and PG content of the injured tissue. Pre-trauma cyclic loading increases the PG content and stiffness of the cartilage explants (Wei et al., 2008), and increases glcN-CS incorporation in the tissue (Wei and Haut, 2009). However, the effects of post-traumatic cyclic loading have yet to be elicited. The following chapter will focus on the effects of post-traumatic cyclic loading as a potential means of increasing PG synthesis and helping to maintain homeostasis of the damaged cartilage by enhancing the effect of glcN-CS.

References

Baars, D.C., Rundell, S.A., Haut, R.C. (2006) Treatment with the non-ionic surfactant poloxamer P188 reduces DNA fragmentation in cells from bovine chondral explants exposed to injurious unconfined compression. *Biomechan Model Mechanobiol* **5**, 133-139.

Bank, R.A., Soudry, M., Maroudas, A., Mizrahi, J., TeKoppele, J.M. (2000) The increased swelling and instantaneous deformation of osteoarthritic cartilage is highly correlated with collagen degradation. *Arthritis and Rheumatism* **43**, 2202-2210.

Daniel, D.M., Stone, M.L., Dobson, B.E., Fithian, D.C., Rossman, D.J., Kaufman, K.R. (1994) Fate of the ACL injured patient: a prospective outcome study. *The American Journal of Sports Medicine* **22**, 632-644.

Dodge, G.R. and Jimenez, S.A. (2003) Glucosamine sulfate modulates the levels of aggrecan and matrix metalloproteinase-3 synthesized by cultured human osteoarthritis articular chondrocytes. *Osteoarthritis and Cartilage* **11**, 424-432.

Fang, C., Johnson, D., Leslie, M.P., Carlson, C.S., Robbins, M., Di Cesare, P.E. (2001) Tissue distribution and measurement of cartilage oligomeric matrix protein in patients with magnetic resonance imaging-detected bone bruises after acute anterior cruiate ligament tears. *Journal of Orthopaedic Research* **19**, 634-641.

Felson, D.T. (2004) An update on the pathogenesis and epidemiology of osteoarthritis. *Radiol Clin North Am* **42**, 1-9.

Gillquist, J., Messner, K., (1999) Anterior cruciate ligament reconstruction and the long term incidence of gonarthrosis. *Sports Medicine* **27**, 143-156.

Golenberg, N., Kepich, E., Haut, R.C., (2009) Histomorphological and mechanical property correlations in rabbit tibial plateau cartilage based on a fibril-reinforced biphasic model. *International Journal of Experimental and Computational Biomechanics* **1**, 58-75.

Huser, C.A.M., Davies, M.E. (2006) Validation of an in vitro single-impact load model of the initiation of osteoarthritis-like changes in articular cartilage. *Journal of Orthopaedic Research* **24**, 725-732.

Jeffrey, J.E., Gregory, D.W., Aspden, R.M. (1995) Matrix damage and chondrocyte viability following a single impact load on articular cartilage. *Archives of Biochemistry and Biophysics* **322**, 87-96.

Johnson, D.L., Urban, W.P., Caborn, D.N.M., Vanarthos, W.J., Carlson, C.S. (1998) Articular cartilage changes seen with magnetic resonance imagine-detercted bone bruises associated with acture anterior cruiate ligament rupture. *The American Journal of Sports Medicine* **26**, 409-414.

Khalsa, P.S., Eisenberg, S.R. (1997) Compressive behavior of articular cartilage is not completely explained by proteoglycan osmotic pressure. *Journal of Biomechanics* **30**, 589-594.

Kurz, B., Jin, M., Patwari, P., Cheng, D.M., Lark, M.W., Grodzinsky, A.J. (2001) Biosynthetic response and mechanical properties of articular cartilage after injurious compression. *Journal of Orthopaedic Research* **19**, 1140-1146.

Lin, P.M., Chen, C.-T.C., Torzilli, P.A. (2004) Increased stromelysin-1 (MMP-3), proteoglycan degradation (3B3- and 7D4) and collagen damage in cyclically load-injured articular cartilage. *Osteoarthritis and Cartilage* **12**, 485-496.

Lippiello, L. (2003) Glucosamine and chondroitin sulfate: biological response modifiers of chondrocytes under simulated conditions of joint stress. *OsteoArthritis and Cartilage* **11**, 335-342.

Loening, A.M., James, I.E., Levenston, M.E., Badger, A.M., Frank, E.H., Kurz, B., Nuttall, M.E., Hung, H.-H., Blake, S.M., Grodzinsky, A.J., Lark, M.W. (2000) Injurious mechanical compression of bovine articular cartilage induces chondrocyte apoptosis. *Archives of Biochemistry and Biophysics* **381**, 205-212.

Patwari, P., Kurz, B., Sandy, J.D., Grodzinsky, A.J., (2000) Mannosamine inhibits aggrecanase-mediated changes in physical properties and biochemical composition of articular cartilage. *Archives of Biochemistry and Biophysics* **374**, 79-85.

Phillips, D.M. and Haut, R.C. (2004) The use of non-ionic surfactant (P188) to save chondrocytes from necrosis following impact loading of chondral explants. *Journal of Orthopaedic Research* **22**, 1135-1142.

Richy, F., Bruyere, O., Ethgen, O., Cucherat, M., Henrotin, Y., Reginster, J.-Y. (2003) Structural and symptomatic efficacy of glucosamine and chondroitin in knee osteoarthritis. *Archives of Internal Medicine* **163**, 1514-1522.

Rundell, S.A. (2005) Chapter Three: Glucosamine supplementation can help limit matrix damage and adjacent cell death in traumatized explants. In: *Investigation into the acute injury response of articular cartilage in vitro and in vivo: analysis of various therapeutic treatments*. Theis for the degree of M.S. Michigan State University, 70-95.

Simon, W.H., Richardson, S., Herman, W., Parsons, J.R., Lane, J. (1976) Long-term effects of chondrocyte death on rabbit articular cartilage in vivo. *Journal of Bone and Joint Surgery, Am* **58**, 517-526.

Soulhat, J., Buschmann, M.D., Shirazi-Adl, A. (1999) A fibril-network-reinforced biphasic model of cartilage in unconfined compression. *Journal of Biomechanical Engineering* **121**, 340-347.

Steinmeyer, J., Ackermann, B., Raiss, R.X. (1997) Intermittent cyclic loading of cartilage explants modulates fibronectin metabolism. *Osteoarthritis and Cartilage* **5**, 331-341.

Steinmeyer, J., Knue, S., Raiss, R.X., Pelzer, I. (1999) Effects of intermittently applied cyclic loading on proteoglycans metabolism and swelling behavior of articular cartilage explants. *Osteoarthritis and Cartilage* **7**, 155-164.

Tiraloche, G., Girard, C., Chouinard, L., Sampalis, J., Moquin, L., Ionescu, M., Reiner, A., Poole, A.R., Laverty, S. (2005) Effect of oral glucosamine on cartilage degradation in a rabbit model of osteoarthritis. *Arthritis and Rheumatism* **52**, 1118-1128.

Torzilli, P.A., Grigiene, R., Borrelli, J. Jr., Helfet, D.L. (1999) Effect of impact load on articular cartilage: cell metabolism and viability, and matrix water content. *Journal of Biomechanical Engineering* **121**, 433-441.

Wei, F., Golenberg, N., Kepich, E.T., Haut, R.C. (2008) Effect of intermittent cyclic preloads on the resoponse of articular cartilage explants to an excessive level of unconfined compression. *Journal of Orthopaedic Research* **26**, 1636-1642.

Wei, F. and Haut, R.C. (2009) High levels of glucosamine-chondroitin sulfate can alter the cyclic preload and acute overload responses of chondral explants. *Journal of Orthopaedic Research* **27**, 353-359.

Chapter 4

Investigation of low level cyclic loading following high levels of unconfined compression with and without glucosamine chondroitin sulfate treatment

Abstract

A defining feature of OA is softening of the articular cartilage and decreased tissue proteoglycan (PG) content. Low level cyclic loading has been shown to increase matrix stiffness and cell biosynthesis, specifically PG synthesis, and increase incorporation of glcN-CS. The hypothesis of the current study was that the matrix stiffness and tissue PG content would increase with cyclic loading post-trauma and that the glcN-CS effect previously documented would be further enhanced with low level cyclic loading post-trauma. Bovine chondral explants were subjected to 10 or 25 MPa of unconfined compression followed by 0.5 MPa of cyclic loading. Treatment with glcN-CS was also investigated. An increase in PG content was documented with glcN-CS treatment and cyclic loading following both 10 MPa and 25 MPa of unconfined compression compared to cyclic loading alone. No difference in the matrix modulus was documented with glcN-CS treatment following either level of unconfined compression. Previous studies have documented that the elastic properties of cartilage are influenced by the aggregate structure of the proteoglycans, not only their tissue content. Proteoglycans from degenerated tissue cartilage were found to be smaller and had lost their ability to bind to hyaluronic acid and form aggregates. Therefore, future studies are still needed to study the type and shape of the proteoglycans produced by injured cells following unconfined compression with the additional stress associated with cyclic loading.

Introduction

Injuries during participation in sports, recreation, and exercise (SRE) have been associated with long-term development of osteoarthritis (OA) (Lane, 1996). A defining feature of OA is softening of the articular cartilage and decreased tissue proteoglycan (PG) content. Matrix PGs are responsible for cartilage resistance to stress and strain and the loss of mechanical stiffness in OA tissue is suggested to be caused by decreased PG content (Patwari et al., 2000). The prevention of PG loss following traumatic injury has also been suggested as a possible intervention aimed at the prevention of post-traumatic OA. While treatments of OA are currently limited, mechanical stimulation and nutraceutical treatments, such as glucosamine-chondroitin sulfate (glcN-CS), have been investigated as possible means of repairing articular cartilage and increasing matrix PG content following traumatic injury.

Low to moderate levels of exercise increase PG synthesis and increase the matrix stiffness of articular cartilage. Clinically, following regular exercise, patients previously diagnosed with high risk of developing knee OA saw an increase in PG content (Roos and Dahlberg, 2005). Similarly, *in vivo* animal models have been used to document increases in matrix PGs and tissue stiffness with exercise. A previous study using a canine model documents an increase in the tissue PG content, specifically in regions of high loading following regular exercise (Kiviranta et al., 2005). A study by Jurvelin et al. (1986) also documents that regular exercise increases compressive stiffness in canine articular cartilage. A post-traumatic study using a Flemish Giant rabbit model documents that exercise prevents the loss of matrix PGs (Weaver and Haut, 2005).

In vitro studies have also been used to investigate the effects of low level (0.5-5 MPa) mechanical loading on articular cartilage. Low level cyclic loading increases cell biosynthesis, specifically PG synthesis (Torzilli et al., 1999; Sah et al. 1989; Millward-Sadler and Salter, 2004). Wei et al. (2008), using bovine chondral explants, document that 0.5 MPa of cyclic loading over 14 days results in an increase in tissue matrix modulus and decreases the tissue permeability. This increase in mechanical stiffness is correlated with an increase in matrix PGs and results in a decrease in the severity and extent of surface fissures and cell death in the tissue. Moreover, low level cyclic loading increases the incorporation of glcN-CS throughout the tissue and results in a further increase in PG content and mechanical stiffness of cartilage (Wei and Haut, 2009, Sharma et al., 2008).

The previous chapter documented the ability of glcN-CS to increase matrix PG content and matrix stiffness following 10 MPa and 25 MPa of unconfined compression and pre-trauma cyclic loading further increases glcN-CS incorporation. However, post-traumatic cyclic loading of cartilage explants has not been documented. Therefore, the purpose of the current study was to determine whether low level cyclic loading would increase the mechanical stiffness of cartilage explants post-trauma and investigate if cyclic loading will enhance the incorporation and effects of glcN-CS documented in the previous chapter. The hypothesis of the current study was that the matrix stiffness and tissue PG content would increase with exercise and that the glcN-CS effect previously documented would be further enhanced with low level cyclic loading post trauma.

Method

Dissection and tissue culture

Skeletally mature bovine forelegs were obtained from a local abattoir within 2 hours of slaughter. The legs were rinsed with water and skinned prior to exposing the metacarpal joint under a laminar flow hood. A 6 mm diameter biopsy punch (Miltex Instrument Company, Bethpage, NY) was used to make chondral explants from the lower metacarpal surface of the limbs. Each explant was separated from the underlying bone with a scalpel. The explants were randomly assigned to two impact load groups (10 MPa and 25 MPa). Each of these groups was further divided into two sub groups, with and without glcN-CS treatment: '10 MPa with glcN-CS' (n=8), '10 MPa without glcN-CS' (n=12), '25 MPa with glcN-CS' (n=8), and '25 MPa without glcN-CS' (n=12). All specimens were washed three times in Dulbecco's Modified Eagle Media: F12 (DMEM: F12) (Gibco, USA, #12500-039) supplemented with additional amino acids and antibiotics (penicillin 100 U/ml, streptomycin 1 μg/ml, amphotericin B 0.25 μg/ml). The explants were then incubated in media supplemented with 10% fetal bovine serum in a 24-well plate. Glucosamine and chondroitin sulfate treated samples were placed in a 24-well plate with media supplemented with glucosamine (500 μg/mL (FCHG49®)), chondroitin sulfate (250 μg/mL CS (TRH122®)) (Rundell, 2005; Wei et al., 2008), and 10% fetal bovine serum. The concentration of glcN-CS was chosen to maximize effect of glcN-CS treatment based on previous studies by this laboratory (Rundell, 2005; Wei et al., 2008). The media was replaced every 2 days for the duration of the study. Following initial indentation and unconfined compression at either 10 MPa or 25 MPa, the well plates were placed in a mechanical loading device (the 'cartilage exerciser' (described

below)) inside of a humidity-controlled incubator (37°C, 5% CO_2, 95% humidity). The osmolarity of the media was 300mosM (Osmete 2, Precision Systems), and the pH was 7.4 as this results in physiological and metabolic stability of the explants (Phillips and Haut 2004; Baars et al. 2006; Wei et al. 2008; Wei and Haut 2009).

Indentation testing of the explants

The samples were allowed to equilibrate for 24 hours after harvesting. Prior to unconfined compression, each explant was subjected to an indentation stress relaxation test. Mechanical tests were also performed 7, 14, and 21 days after impact. Before each indentation test, the cartilage explant thickness was measured twice at perpendicular orientations across the center of the explant using a digital vernier caliper (Mitutoyo Corp.: Absolute Digimatic, Model No. CD-6" CS) with a resolution of 0.01 mm (Steinmeyer et al. 1997 and 1999). The two thickness values were then averaged. The explants were then placed on a flat level surface so that the face of the explant was perpendicular to the indenter tip (Figure 4.1b). A magnet with a 4.3 mm diameter hole was placed on top of the explant to secure the edges and help resist curling of the explants (Figure 4.1c). The explant and fixture were then submerged into a room-temperature phosphate buffered saline (PBS with pH 7.2) (Figure 4.1a). A 2.39 mm diameter spherical, non-porous probe was lowered into the cartilage until a preload of 0.05 N was attained and held for 60 s (Figure 4.1d). The indenter was then pressed into the cartilage 25% its total thickness in 2 s and maintained for 600 s while resistive loads of relaxation were measured (Data Instruments, Acton, MA: model JP-25, 25 lb capacity), amplified and collected at 1,000 Hz for the first second and 20 Hz, thereafter.

The stress relaxation curves were obtained and fitted with a fibril-reinforced biphasic finite element model (Soulhat et al. 1999) with an assumed Poisson's ratio of 0.25. Cartilage matrix modulus (E_m), fiber modulus (E_f) and tissue permeability (k_0) were evaluated with a custom-written Gauss-Newton constrained nonlinear least square minimization procedure.

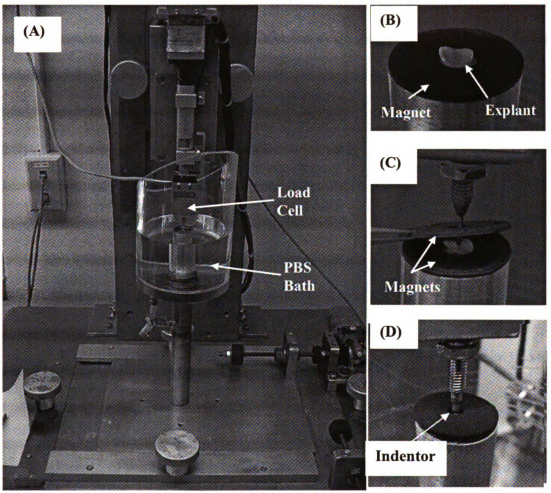

Figure 4.1. Explant indentation test system and fixture (A). The explants were placed in a hold of the bottom magnet on a flat steel surface (B). A top magnet was lowered over the top of the explant to hold down the edges (C). The indentor tip was lowered to a preload of 0.05 N (D).

Unconfined compression tests on the explants

Following a 5 N preload, the explants were taken to either 282 N (~10 MPa) or 707 N (~25 MPa) in unconfined compression between two polished stainless steel plates (Figure 4.2). A 0.5 Hz (1 s time to peak) haversine loading protocol was programmed for application onto the explants in a servo-controlled hydraulic testing machine (Instron, model 1331, retrofitted with 8500 plus electronics, Canton, MA). Immediately after this load protocol, the explants were placed in the 'cartilage exerciser' for the remainder of the study.

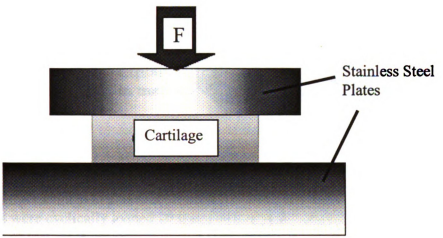

Figure 4.2. Cartilage explants were loaded in unconfined compression at either 10 MPa or 25 MPa between two polished stainless steel plates.

Cyclic loading of the explants

All samples were cyclically loaded for the duration of the study. The 'cartilage exerciser' consisted of 12 loading chambers simultaneously powered by air. Pneumatic cylinders forced the pistons downward to apply a compressive load to the specimens through 14.6 mm diameter non-porous Teflon® platens. The "cartilage exerciser" was designed to hold a 24-well culture plate with 12 cartilage samples that could be mechanically loaded (Figure 4.3). Intermittent, uniaxial cyclic loads were applied using a

0.2 Hz sinusoidal waveform with a peak stress of 0.5 MPa. The cyclic loads were applied for 10 cycles followed by a load-free period lasting 3600 s. During the period of unloading the load platen was lifted from the cartilage surface.

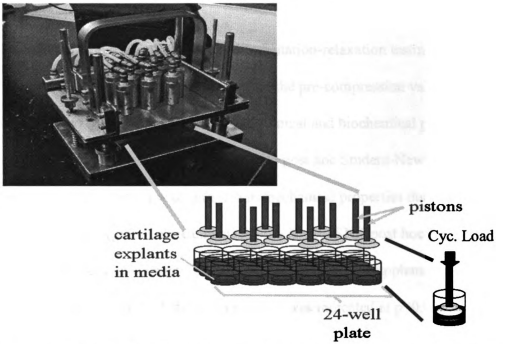

Figure 4.3. The "cartilage exerciser" mechanical loading device applied compressive loads to the cartilage explants in 12 separate loading chambers in a 24 well plate. The samples were cyclically loaded 10 times with a peak stress of 0.5 MPa followed by 3600 seconds of rest. This protocol was then repeated for the duration of the test.

Determination of the tissue proteoglycan (PG) content

Following the 21-day test period, samples were weighed and digested overnight at 60° C in a papain solution. Approximately, 4.5 mg chondroitin sulfate A sodium salt from bovine trachea (Sigma-ALDRICH GmbH Steinheim, Germany) was digested using the same protocol and was used as the standard during this assay. Papain digested cartilage explants and the chondroitin sulfate standards were dimethyl-methylene blue (DMB) assayed for sulfated PGs by the reaction with 1,9-DMB dye solution in

polystyrene 96 well plates and quantitated with spectrophotometry at wavelength 530 nm using a Bio Tek microplate reader.

Statistical Analysis

Mechanical data was collected during indentation-relaxation testing. Post-compression mechanical data were normalized by the pre-compression values. Statistical analysis was used to evaluate differences in mechanical and biochemical properties. A two-factor (day, glcN-CS treatment) ANOVA with post hoc Student-Newman-Keuls (SNK) test was used to determine differences in mechanical properties due to glcN-CS treatment. A one-factor (glcN-CS treatment) ANOVA with SNK post hoc test was used to determine differences in PG content of supplemented and non-supplemented samples at the various loading levels. Statistical significance was indicated at $p<0.05$.

Results

A 20% decrease in the matrix modulus was documented following 10 MPa of unconfined compression and exercise. This decrease in matrix modulus was not changed with glcN-CS treatment (Figure 4.4a). Similarly, a decrease in the matrix modulus was documented following 25 MPa of unconfined compression and exercise. With glcN-CS treatment, however, a statistical trend was noted for an increase in the matrix modulus at 7 ($p=0.055$) and 21 ($p=0.1$) days post trauma (Figure 4.4b). Treatment with glcN-CS increased the PG content in the tissue following 10 ($p=0.027$) and 25 MPa ($p=0.05$) of unconfined compression and post-trauma low level cyclic loading (Figure 4.5).

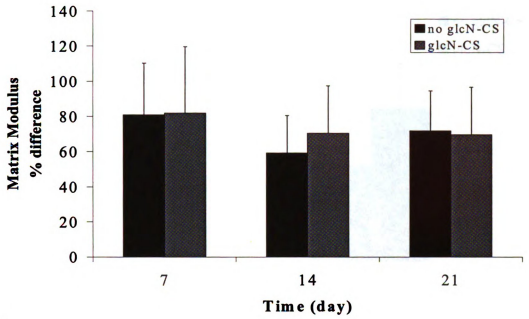

a)

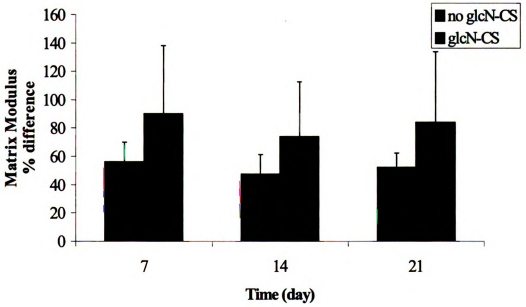

b)

Figure 4.4. The matrix modulus following 10 MPa (a) and 25 MPa (b) of unconfined compression and low level cyclic loading with and without treatment with glcN-CS supplement. No differences were documented with the treatment of glcN-CS following 10 MPa of unconfined compression, while an increase was documented following 25 MPa of unconfined compression and cyclic loading with glcN-CS treatment.

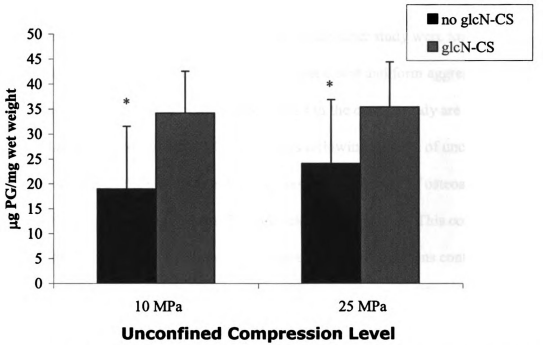

Figure 4.5. PG content of samples with and without glcN-CS supplement. A significant increase in the tissue PG content was documented with the treatment of glcN-CS. '*' denotes a statistically significant difference compared to samples treated with glcN-CS.

Discussion

Previous studies have documented the ability of glcN-CS to increase PG synthesis in cartilage (Lippiello, 2003, Chapter 2). Treatment with cyclic loading and glcN-CS in the current study increased the PG content following both 10 MPa and 25 MPa of unconfined compression compared to cyclic loading alone. Treatment with glcN-CS and cyclic loading after trauma also increased the matrix stiffness of samples loaded with 25 MPa of unconfined compression, which supported the findings from Chapter 2 of this thesis. Interestingly, while glcN-CS with cyclic loading after trauma was found to increase the PG content in the tissue following 10 MPa of unconfined compression, there was no tendency for an increase in the matrix stiffness of the tissue. Previous studies have documented that the elastic properties of cartilage are influenced by the aggregate

structure of the proteoglycans, not only their tissue content (Inerot and Heinegard, 1978). Proteoglycans from degenerated tissue cartilage in the latter study were found to be smaller and had lost their ability to bind to hyaluronic acid and form aggregates. While the size and binding potential of the proteoglycans in the current study are unknown, it is possible that the proteoglycans produced by cells following 10 MPa of unconfined compression with cyclic post trauma loading may resemble those of osteoarthritic cartilage previously shown to be smaller and lacking binding sites. This could help explain the lack of a correlation between changes in the proteoglycans content of the tissue exposed to 10 MPa with cyclic loading and its mechanical stiffness. The lower level loading may have damaged significant number of cells causing a significant level of cellular dysfunction in the tissue. In contrast after 25 MPa of compression, the damaged cells may have lost any degree of viability even to produce these dysfunctional PGs.

Previous studies by Wei et al. (2008) document an increase in PG content and matrix stiffness with low level cyclic loading. However, a comparison with the previous chapter revealed no significant changes in matrix stiffness with cyclic loading following both 10 and 25 MPa of unconfined compression (Figure 4.6) along with no significant changes in PG content of the tissue with or without the cyclic loading post-trauma (Figure 4.7). A study by Kurz et al. (2001) documents that cells that are mechanically injured may not be able to respond to dynamic mechanical stimulation either because the cells have lost the ability to do so or because damage to the extracellular matrix has disrupted the transduction of physical signals to the cells.

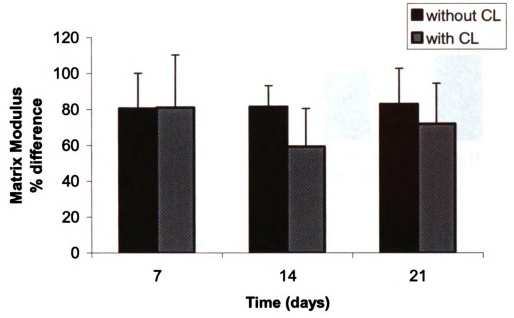

a)

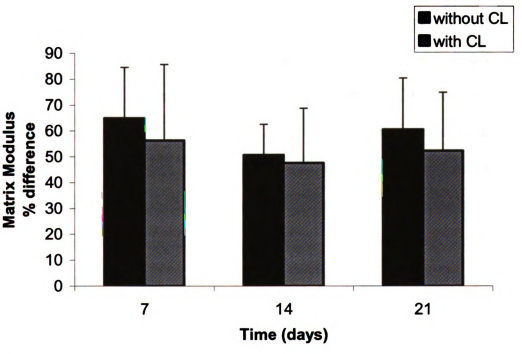

b)

Figure 4.6. The matrix modulus following 10 MPa (a) and 25 MPa (b) of unconfined compression with and without exercise (from Chapter 2). No differences were documented due to cyclic loading in either of the loading groups.

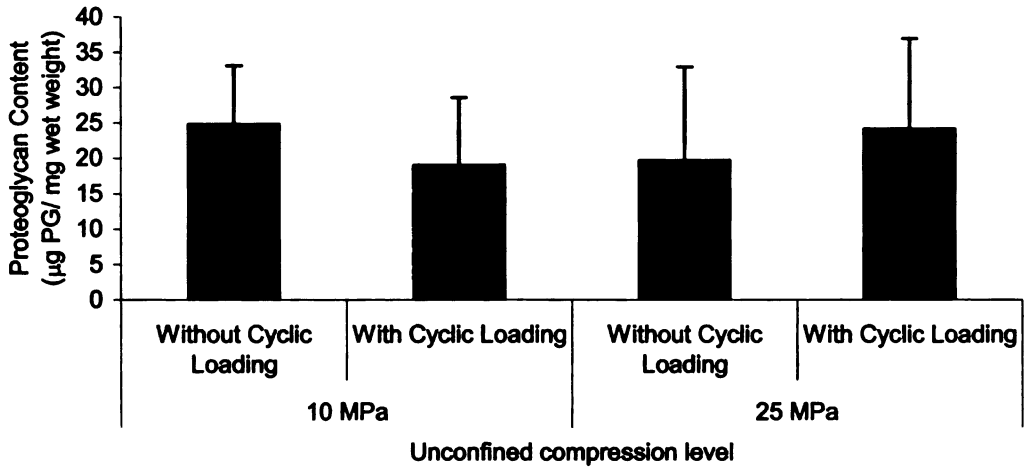

Figure 4.7. The PG content following 10 MPa and 25 MPa of unconfined compression with and without cyclic loading. No significant differences were documented between the samples with or without cyclic loading.

Multiple factors are associated with the cartilage properties. Cell viability depends on loading levels and loading rates (Torzilli et al., 1999; Loening et al., 2000). Additionally, the loading levels and loading rates alter the mechanical integrity (Kurz et al., 2001) of the cartilage as well as effect cellular biosynthesis (Wilkins et al., 2000). Furthermore, these mechanical stimulations affect the level of pharmaceutical efficacy (Sah et al., 1989). Therefore, future studies should continue to focus on multiple loading situations and their effects on changes in chondrocyte biosynthesis and cartilage integrity. The exact mechanism that inhibited the increase in the matrix stiffness is currently unknown, therefore, future studies are still needed to study the type and shape of the proteoglycans produced by injured cells following unconfined compression with the additional stress associated with cyclic loading. Additional studies will also be needed to investigate both cellular viability and cellular synthesis alterations with glcN-CS treatments in combination with cyclic loading on mechanically injured cartilage.

References

Baars, D.C., Rundell, S.A., Haut, R.C. (2006) Treatment with the non-ionic surfactant poloxamer P188 reduces DNA fragmentation in cells from bovine chondral explants exposed to injurious unconfined compression. *Biomechan Model Mechanobiol* **5**, 133-139.

Inerot, S., and Heinegard, D. (1978) Articular-cartilage proteoglycans in aging and osteoarthritis. *Biochem. J.* **169**, 143-156.

Jurvelin, J., Kiviranta, I., Tammi, M., Helminen, H.J., (1986) Effect of physical exercise on indentation stiffness of articular cartilage in the canine knee. *Int. J. Sports Med.* **7**, 106-110.

Kiviranta, I., Tammi, M., Jurvelin, J., Saamanen, A.-M., Helminen, H.J. (2005) Moderate running exercise augments glycosaminoglycans and thickness of articular cartilage in the knee joint of young beagle dogs. *Journal of Orthopaedic Research* **6**, 188-195.

Kurz, B., Jin, M., Patwari, P., Cheng, D.M., Lark, M.W., Grodzinsky, A.J. (2001) Biosynthetic response and mechanical properties of articular cartilage after injurious compression. *Journal of Orthopaedic Research* **19**, 1140-1146.

Lane, N. (1996) Physical activity at leisure and risk of osteoarthritis. *Annals Rheumatic Disease* **55**, 682-684.

Lippiello, L. (2003) Glucosamine and chondroitin sulfate: biological response modifiers of chondrocytes under simulated conditions of joint stress. *OsteoArthritis and Cartilage* **11**, 335-342.

Loening, A.M., James, I.E., Levenston, M.E., Badger, A.M., Frank, E.H., Kurz, B., Nuttall, M.E., Hung, H.-H., Blake, S.M., Grodzinsky, A.J., Lark, M.W. (2000) Injurious mechanical compression of bovine articular cartilage induces chondrocyte apoptosis. *Archives of Biochemistry and Biophysics* **381**, 205-212.

Millward-Sadler, S.J., Salter, D.M. (2004) Integrin-dependent signal cascades in chondrocyte mechanotransduction. *Annals of Biomedical Engineering* **32**, 435-446

Patwari, P., Kurz, B., Sandy, J.D., Grodzinsky, A.J., (2000) Mannosamine inhibits aggrecanase-mediated changes in physical properties and biochemical composition of articular cartilage. *Archives of Biochemistry and Biophysics* **374**, 79-85.

Phillips, D.M. and Haut, R.C. (2004) The use of non-ionic surfactant (P188) to save chondrocytes from necrosis following impact loading of chondral explants. *Journal of Orthopaedic Research* **22**, 1135-1142.

Roos, E.M. and Dahlberg, L. (2005) Positive effects of moderate exercise on glycosaminoglycan content in knee cartilage: A four-month, randomized, controlled trial in patients at risk of osteoarthritis. *Arthritis and Rheumatism* **52**, 3507-3514.

Rundell, S.A. (2005) Chapter Three: Glucosamine supplementation can help limit matrix damage and adjacent cell death in traumatized explants. In: *Investigation into the acute injury response of articular cartilage in vitro and in vivo: analysis of various therapeutic treatments*. Theis for the degree of M.S. Michigan State University, 70-95.

Sah R.L.-Y., Kim, Y.-J., Doong, J.-Y.H., Grodzinsky, A.J., Plaas, A.H.K., Sandy, J.D. (1989) Biosynthetic response of cartilage explants to dynamic compression. *Journal of Orthopaedic Research* **7**, 619-636.

Sharma, G., Sazena, R.K., Mishra, P. (2008) Synergistic effect of chondroitin sulfate and cyclic pressure on biochemical and morphological properties of chondrocytes from articular cartilage. *Osteoarthritis and Cartilage* **16**, 1387-1394.

Soulhat, J., Bsuhmann, M.D., Shirazi-Adl, A. (1999) A fibril reinforced biphasic model of cartilage in unconfined compression. *Journal of Biomechanical Engineering* **121**, 340-347.

Steinmeyer, J., Ackermann, B., Raiss, R.X. (1997) Intermittent cyclic loading of cartilage explants modulates fibronectin metabolism. *Osteoarthritis and Cartilage* **5**, 331-341.

Steinmeyer, J., Knue, S., Raiss, R.X., Pelzer, I. (1999) Effects of intermittently applied cyclic loading on proteoglycans metabolism and swelling behavior of articular cartilage explants. *Osteoarthritis and Cartilage* **7**, 155-164.

Torzilli, P.A., Grigiene, R., Borrelli, J. Jr., Helfet, D.L. (1999) Effect of impact load on articular cartilage: cell metabolism and viability, and matrix water content. *Journal of Biomechanical Engineering* **121**, 433-441.

Weaver, B.T., and Haut, R.C. (2005) Enforced exercise after blunt trauma significantly affects biomechanical and histological changes in rabbit retro-patellar cartilage. *Journal of Biomechanics* **38**, 1177-1183.

Wei, F., Golenberg, N., Kepich, E.T., Haut, R.C. (2008) Effect of intermittent cyclic preloads on the response of articular cartilage explants to an excessive level of unconfined compression. *Journal of Orthopaedic Research* **26**, 1636-1642.

Wei, F. and Haut, R.C. (2009) High levels of glucosamine-chondroitin sulfate can alter the cyclic preload and acute overload responses of chondral explants. *Journal of Orthopaedic Research* **27**, 353-359.

Wilkins, R.J., Browning, J.A., Urban, J.P.G. (2000) Chondrocyte regulation by mechanical load. *Bioheology* **37**, 67-74.

Chapter 5

Effects of acute repair of chondrocytes in the rabbit tibio-femoral joint 6 weeks following blunt impact using P188 surfactant

Abstract

Recent studies have indicated that there may be a correlation between acute chondrocyte damage and joint degeneration reminiscent of early stage OA. P188 surfactant has been shown to acutely restore the integrity of damaged chondrocytes; however, its long term efficacy is unknown. The hypothesis of this study was that a single injection of P188 into a traumatized joint would acutely repair damaged cell membranes and maintain their viability in the longer term. Six rabbits were divided into two groups, with and without P188 treatment and sacrificed after 6 weeks post-trauma. P188 treatments were administered immediately post-trauma. A decrease in the density of viable cells was documented in the untreated impacted limb versus its contralateral control, while no difference in the density of viable cells was documented in the impacted treated limb versus its contralateral control. The results of the current study confirm the acute efficacy of P188 treatment in the longer term, but, additional studies are still needed to investigate the chronic implications of the acute repair of cells on the traumatized joint.

Introduction

Participation in sports, recreation, and exercise (SRE) is becoming increasingly popular and widespread in today's culture. Participation in SRE increases the risk of acute and chronic injuries such as ligament tears and osteoarthritis (OA), respectively (Lane, 1996). Knee joint injuries, such as cruciate ligament damage and meniscal tears (Felson, 2004), have been associated with excessive compressive forces passing through the joint causing damage to the articular cartilage. Specifically, damage to the anterior cruciate ligament (ACL) leads to characteristic osteochondral lesions in the postero-lateral aspect of the tibia and/or antero-lateral aspect of the lateral femoral chondyle (Atkinson et al., 2008). Of concern in the current literature is evidence of damage to articular cartilage and chondrocytes in regions overlying these bone bruises. Since 50% of ACL tear patients develop radiological signs of OA within ten years following injury with or without ACL reconstruction, acute injury to the cartilage and subchondral bone may play an important role in the progression of chronic joint disease.

Death of chondrocytes following traumatic injury has been hypothesized to be associated with the long-term development of OA as cell death has been correlated with degeneration of the cartilage matrix (Hashimoto et al., 1998, Duda et al., 2001, Simon et al., 1996). These degenerative changes result in a loss of tissue integrity, represented by a decrease in tissue stiffness, and an increase in tissue permeability (Kurz et al., 2001; Ewers and Haut, 2000; Ewers et al., 2001). A study using the porcine patella documents considerable cellular dysfunction that may act to promote subsequent structural tissue damage (Duda et al., 2001). This may be particularly important because the synthesis of cartilage matrix proteins is directly dependant on cell viability and homeostasis (Duda et

al., 2001). Since chondrocytes are required for matrix repair and chondrocyte death leads to matrix loss, chondrocyte death and repair has become a focus of OA research and more recently cartilage trauma research.

A defining feature of cellular necrosis is swelling of the cell due to a damaged membrane. Damage to the plasma membrane allows an influx of fluid into the cell resulting in the inability of the cell to maintain an ionic gradient. As a result the cell swells and eventually ruptures (Duke et al., 1996). Surfactants, such as poloxamer P188 (P188), interact with this damaged cell membrane. P188 is an 8400-dalton triblock copolymer containing both hydrophobic and hydrophilic regions. Marks et al. (2001) shows that P188 surfactant specifically inserts into only the damaged areas of a cell membrane. Studies by our laboratory, and others, have shown P188 to be effective in reducing the loss of chondrocyte in articular cartilage following traumatic loading to the PF joint (Rundell et al., 2005) and TF joint (Isaac et al., in review). Additionally, studies have documented the ability of P188 to repair membrane damage and increase cell viability in bovine chondral (Baars et al., 2006) and osteochondral explants (Natoli and Athanasiou, 2008).

Because of the growing interest in SRE, and the increasing number of injuries to the TF joint, the current study focuses on the effects of a single traumatic load to the rabbit TF joint. Previous studies have documented increases in cell viability acutely with P188 treatment; however, to my knowledge this is the first study to investigate long term efficacy of P188. The hypothesis of the current study was that a single injection of P188 into the rabbit TF joint following traumatic injury would acutely repair the damaged cell membrane and its efficacy will be validated by a long term increase in the density of

viable cells.

Materials and Methods

Impact

Six skeletally mature Flemish Giant rabbits aged 6-12 months (5.6 ± 0.2 kg) were used in this study after approval by an All-University Committee on Animal Use and Care. All rabbits were housed in individual cages (152 x 152 x 36 cm) and allowed free cage activity for this study. Using a previously described impact method, a 1.75 kg mass with a pre-crushed, deformable impact head (Hexcel, 3.76 MPa crush strength) was dropped onto the left tibio-femoral (TF) joint of the anesthetized rabbit (2% isoflurane and oxygen) (Isaac et al. 2008). The right limb served as an unimpacted control. The impact interface was mounted in front of a 4.45 kN (1000 lb.) load transducer (Model AL311CV, 1000 lb capacity, Sensotec, Columbus, Ohio) (Figure 5.1). The mass was arrested electronically after the first impact, avoiding multiple loadings on the joint.

The animals were randomly divided into two groups, 'P188' (n=3) and 'no P188' (n=3). The 'P188' animals received a 1.5 mL injection of P188 at 8 mg/mL concentration (Rundell et al., 2005) in sterile phosphate buffered saline (PBS) into the left, impacted joint. The right limb received a 1.5 mL sham sterile PBS injection. The 'no P188' rabbits received a 1.5 mL sham injection into both limbs. The combination of P188 in PBS and PBS sham solutions were filter sterilized prior to injection using a 0.2 mm vacuum filter (Nalgene, Nalge Nunc Int., Rochester, NY). To insure distribution of the injection into the joint, the limb was manually flexed a number of times following the treatment.

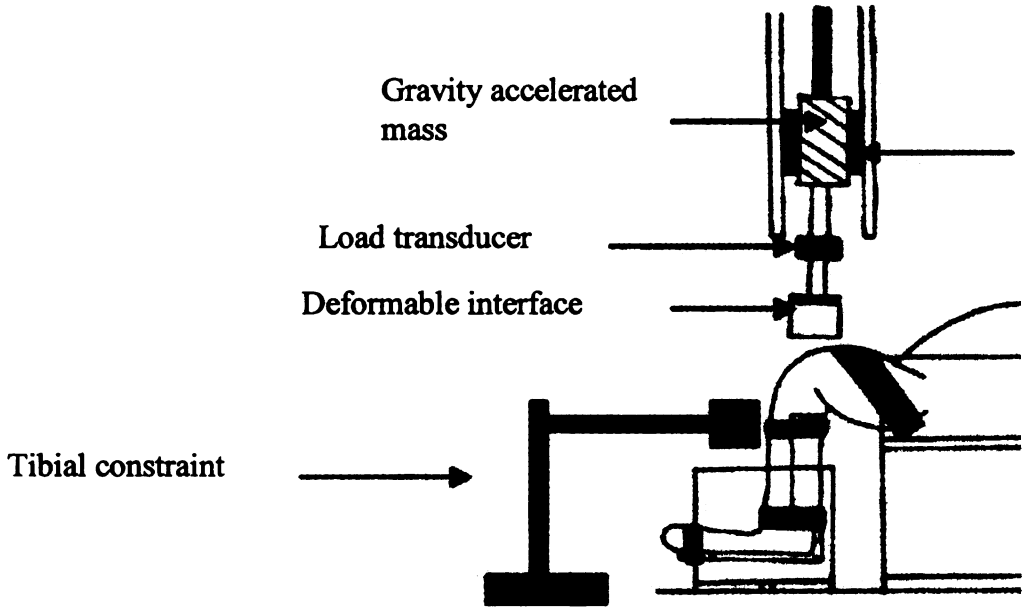

Figure 5.1. Impact experiments were conducted by dropping a gravity-accelerated mass onto the flexed knee so that impacts were isolated on the TF joint.

Dissection and Harvesting

The animals were sacrificed 6 weeks following impact with 85.9 mg/kg BW Pentobarbital IV. The joint was dissected immediately after sacrifice, and examined for abnormalities. The medial (MTP) and lateral (LTP) tibial plateaus were then prepared for cell viability analyses. A 6 mm trephine (TREPH-6, Salvin Dental Specialties, Charlotte, NC) was used to core a region of the MTP and LTP in areas not covered by the menisci, as these were determined to be regions of high contact pressure during impact (Isaac et al., 2008). The cores were undercut using a diamond saw (Isomet 11-1180 Low Speed Saw, Buehler, Lake Bluff, IL) leaving approximately 0.5 mm of bone underlying the articular cartilage. Coronal slices were taken across the medial (MFC) and lateral (LFC) femoral chondyles in a predetermined area of interest leaving approximately 0.5 mm of bone underlying the articular cartilage. All explants were washed three times in

Dulbecco's Modified Eagle Media: F12 (DMEM: F12) (Gibco, USA, #12500-039) supplemented with additional amino acids and antibiotics (penicillin 100 U/ml, streptomycin 1 μg/ml, amphotericin B 0.25 μg/ml), and placed in this supplemented media with 10% fetal bovine serum in a 24-well plate. The samples were allowed to incubate for 24 hours in a humidity-controlled incubator (37 C, 5% CO2, 95% humidity).

Cell viability

Following incubation, a specialized cutting device was used to obtain full thickness sections of the explants for cell viability analyses (Ewers et al., 2001) (Figure 5.2). Prior to staining, the slices were rinsed three times with PBS. The slices were then stained with calcein AM and ethidium homodimer (EthD-1), according to the manufacturer's specifications (Live/Dead Cytotoxicity Kit, Molecular Probes, Eugene, OR). Following the staining, each sample was rinsed three times with PBS to remove any excess stain. The sections were viewed under a fluorescence microscope (Leitz Dialux 20, Leitz Mikroskopie and System GmgH, Wetlzar, Germany). Viable cells were distinguished by the presence of fluorescent calcein AM (green). The presence of a damaged plasma membrane was identified by a bright red fluorescence due to ethidium homodimer penetrating the damaged membrane. The number of viable and damaged cells were manually counted by two blinded readers (DI, NG) using an image analysis program (Image J, National Institutes of Health, 2004). A representative area of each explant was selected. Its thickness and width were measured (Sigma Scan, SPSS Inc., Chicago, IL) and used to calculate the density of cells for each sample.

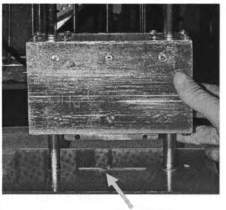

Figure 5.2. A custom cartilage cutting device was used to prepare slices of tissue for cell viability.

Statistical Analysis

A two factor (limb, facet) repeated measures ANOVA with post hoc Student-Newman-Keuls (SNK) test was used to compare the density of viable cells between the left impacted limb and the right unimpacted control of both the treated and untreated animals. A one factor (limb) repeated measures ANOVA was used to document differences between the unimpacted and impacted limb of both the treated and untreated animals. Statistical significance was indicated at $p<0.05$.

Results

Gross inspection of the joints at necropsy showed no signs of joint disease and no damage to ligaments or menisci. No statistical differences were found in the times to peak impact load or the magnitudes of the peak load between treatment groups. The average peak, inertially compensated impact load and impact duration were 1102 ± 92 N and 23.0 ± 0.2 ms, respectively.

Compartmental analyses revealed no statistically significant differences in the

density of viable cells between the impacted and unimpacted limbs of either the 'P188' (Figure 5.3a) or the 'no P188' (Figure 5.3b) rabbits. A statistically significant higher density of viable cells was documented, however, in the right limb (average across facets excluding the medial tibial plateau) compared to the left limb of the 'no P188' rabbits ($p=0.026$) (Figure 5.4). No significant difference was documented in the impacted versus unimpacted limb of the P188 treated rabbits.

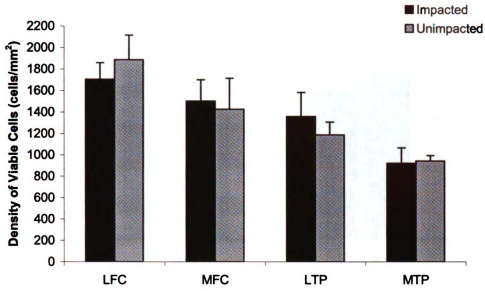

a) treated

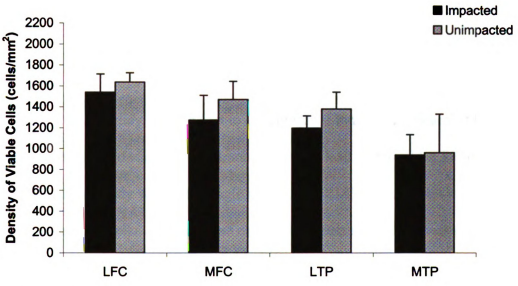

b) untreated

Figure 5.3. No significant differences were documented in the density of viable cells between the impacted and unimpacted limbs in the lateral femoral chondyle (LFC), medial femoral chondyle (MFC), lateral tibial plateau (LTP) or medial tibial plateau (MTP) of the treated (a) and untreated (b) rabbits.

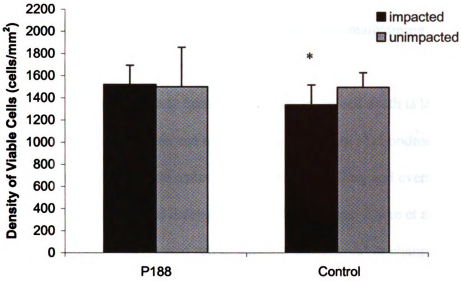

Figure 5.4. Analysis of the impacted and unimpacted limbs revealed a significant difference in the density of viable cells in the 'no P188' group. No significant difference, however, was noted in the 'P188' group. This suggests that P188 had a benefit in preventing the long term degeneration of acutely injured chondrocytes in the TF joint. '*' indicates a statistically significant difference between the impacted and the unimpacted limbs.

Discussion

The current study was the first to document the long term efficacy of P188 on cell membrane repair following a single, traumatic injury load on the rabbit TF joint. The hypothesis of this study was that a single injection of P188 into the joint would acutely repair the damaged cells, and that these cells would remain viable 6 weeks post-trauma. Previous studies document that a 13 J impact to the rabbit TF joint results in a decrease in cell viability 4 days post-trauma (Isaac, 2009). And, that an acute treatment with P188 results in an increase in the density of viable cells 4 days post-trauma. The current study documented a statistical decrease in the viable cell density in the impacted limb versus the contralateral, control limb in the untreated animals ($p=0.026$). On the other hand, no significant difference in the viable cell density was documented in the impacted limb

versus the contralateral, control limb of the P188 treated animals. This analysis supports the previous findings, suggesting that P188 was effective in maintaining viability of acutely repaired cells in the longer-term.

The mechanism that leads from traumatic injury to cell death is largely unknown, although two pathways, necrosis and apoptosis, result in loss of chondrocytes. Cells appear to enter an acute necrotic pathway, undergoing swelling and eventually cellular lysis, following trauma induced damage to the cell membrane (Duke et al., 1996). Excessive mechanical stress causes cell membrane damage and/or changes in membrane transport pathways, such as Na+/K+ pump, which regulate cellular volume (Wilkins et al., 2000). The current study documents cell viability by cell membrane damage, a defining feature of acute necrosis. Apoptosis may have also been initiated in the damaged cells following trauma, but not documented by the current cell viability assays. Apoptotic cells may be documented by TUNEL+ staining. Such cells occur as early as 48 hours after excessive mechanical loading (Chen et al., 2001). The percentage of these cells increases up to 21 days post-trauma in other studies (Clements et al., 2004; Levin et al., 2001). Apoptosis results in the fragmentation of the nucleus which condenses into structures that may contain apoptotic enzymes (Majno and Joris, 1995), such as caspase (D'Lima et al., 2001). These apoptotic enzymes may be released into the matrix and initiate cell apoptosis in viable cells (Levin et al., 2001). A previous study by Natoli and Athanasiou (2008) suggests acute chondrocyte repair using P188 surfactant prevents both apoptotic and necrotic cell death as preventing necrosis may also inhibit the release of apoptotic initiators into the matrix. Apoptosis also is known to cause membrane damage in its later stages (Columbano, 1995). In the current study, all cells with membrane

damage would have been identified as necrotic cells, but some of these may actually be in the late stage of apoptotic death. A previous study by our laboratory documents P188 is effective in preventing apoptotic cell death documented by TUNEL staining in bovine chondral explants 7 days post-trauma (Baars et al. 2006). Since the density of viable cells remained at 'control levels' in the current study, P188 may be effective in preventing both cell death pathways in the longer-term.

A limitation of the current study was the relatively small sample size. Power analyses revealed, on average, approximately 17 animals would be required to attain statistical significance in the density of viable cells between the impacted and contralateral control in the LFC, MFC, and the LTP of untreated animals. On the other hand, because the density of viable cells in the treated limb was actually, on average, greater than the density of viable cells in the contralateral, control, a significantly larger sample size would be required to show fewer viable cells in P188 treated limbs than controls. This suggests greater differences in the untreated rabbit, indicating P188 may have actually restored the density of viable cells closer to 'control levels'. The data from the MTP revealed no differences between the impacted and contralateral, control limb in either the treated or untreated animals. Previous studies have documented that the medial tibial plateau has significantly more baseline damage (Golenberg et al., 2008) and, therefore, excessive loading to the cartilage does not increase the percentage of damaged cells (Isaac, 2009), limiting the efficacy of P188. Therefore, in the above analysis the MTP data has been excluded.

In an attempt to further examine the long term efficacy of P188 in our first study with a limited number of specimens, the data from all compartments of the TF joint were

combined. A previous study by Isaac (2009) has previously documented that P188 was effective in increasing viable cells in all of these compartments. Additionally, all compartments of the joint were subjected to the same testing protocol; therefore, the MFC, LFC, and LTP were combined in this analysis. The analysis revealed a significant decrease in the density of viable cells between the impacted limb and contralateral, control limb of the untreated animals, but no difference was documented in the treated animals. Since the impacted limbs of both the treated and untreated animals were handled in the same manner both during testing and analysis, and a statistical significance was documented in the density of viable cells of the impacted versus contralateral, control limb in the untreated animals but not in the treated animals, the efficacy of P188 may have been established in this current study with this limited number of specimens.

Early signs of OA, such as fissuring, were not documented in either the treated or untreated rabbits of the current study. But, a previous study by Armstrong and Mow (1982) suggests that the visual or histological appearance of the cartilage is a poor indication of its mechanical integrity. The current study suggests that P188 was effective in maintaining the viability of acutely damaged cells 6 weeks post-trauma by repairing the damaged cell membranes, however, the effects of saving these cells on the mechanical integrity of cartilage was not documented. Future studies should focus on the effects that rescuing the cells with P188 has on maintaining the functional stiffness of the cartilage, since this is needed to maintain homeostasis of the joint tissue. Our initial results indicate that pharmacologic approaches, such as treatment with P188 surfactant, directed specifically at the injured cartilage may provide a new approach for decreasing cell damage and helping to ensure the survival of joint cartilage. Damage to the articular

cartilage overlying bone lesions in the ACL tear patient is thought to lead to the development of OA. Treatment with P188 targeting these damaged cells may lead to better outcomes in the surgically repaired patient and possible OA prevention.

Acknowledgments

This study was supported by a grant from the Centers for Disease Prevention and Control, Center for Injury Control & Prevention (CE000623). The contents of this manuscript are solely the responsibility of the authors and do not necessarily represent the official views of the Center for Injury Prevention and Control. The authors wish to acknowledge Ms. Jean Atkinson (J.A.) for her assistance in animal care, Dan Isaac (D.I.) for his assistance in cell viability analyses and impact procedures, and Eric Meyer for his assistance in the impact procedures.

References

Armstrong, C.G. and Mow, V.C. (1982) Variations in the intrinsic mechanical properties of human articular cartilage with age, degeneration, and water content. *The Journal of Bone and Joint Surgery* **64**, 88-94.

Atkinson, P., Cooper, T., Anseth, S., Walter, N., Kargus, R., Haut, R.C. (2008) Association of knee bone bruise frequency with time post-injury and type of soft tissue injury. *Orthop* **31**, 440.

Baars, D.C., Rundell, S.A., Haut, R.C. (2006) Treatment with the non-ionic surfactant poloxamer P188 reduces DNA fragmentation in cells from bovine chondral explants exposed to injurious unconfined compression. *Biomech Model Mechanobiol* **5**, 133-139.

Chen, C.T., Burton-Wurster, N., Borden, C., Hueffer, K., Bloom, S.E., Lust, G. (2001) Chondrocyte necrosis and apoptosis in impact damaged articular cartilage. *J Orthop Res* **19**, 703-711.

Clements, K.M., Burton-Wurster, N., Lust, G. (2004) The spread of cell death from impact damaged cartilage: lack of evidence for the role of nitric oxide and caspases. *Osteoarthritis and Cartilage* **12**, 577-585.

Columbano, A. (1995) Cell death: current difficulties in discriminating apoptosis from necrosis in the context of pathological processes in vivo. *Journal of Cellular Biochemistry* **58**, 181-190.

D'Lima D.D., Hashimoto, S., Chen, P.C., Colwell, C.W. Jr., Lotz, M.K. (2001) Impact of mechanical trauma on matrix and cells. *Clinical Orthopaedics and Related Research* **1**, S90-S99.

Duda, G.N., Eilers, M., Loh, L., Hoffman, J.E., Kaab, M., Schaser, K. (2001) Chondrocyte death precedes structural damage in blunt impact trauma. *Clinical Orthopaedics and Related Research* **393**, 302-309.

Duke, R.C., Ojcius, D.M., Young, J.D. (1996) Cell suicide in heath and disease. *Scientific American* **275**, 80-87.

Ewers, B.J., Haut, R.C. (2000) Polysulphated glycosaminoglycan treatments can mitigate decreases in stiffness of articular cartilage in a traumatized animal joint. *J Orthop Res* **18**, 756-761.

Ewers, B.J., Weaver, B.T., Sevensma, E.T., Haut, R.C., (2001) Chronic changes in rabbit retro-patellar cartilage and subchondral bone after blunt impact loading of the patellofemoral joint. *Journal of Orthopaedic Research* **20**, 545-550.

Felson, D.T. (2004) An update on the pathogenesis and epidemiology of osteoarthritis. *Radiol Clin North Am* **42,** 1-9.

Golenberg, N., Kepich, E., Haut, R.C., (2009) Histomorphological and mechanical property correlations in rabbit tibial plateau cartilage based on a fibril-reinforced biphasic model. *International Journal of Experimental and Computational Biomechanics* **1**, 58-75.

Hashimoto, S., Ochs, R.L., Komiya, S., Lotz, M. (1998) Linkage of chondrocyte apoptosis and cartilage degradation in human osteoarthritis. *Arth Rheum* **41**, 1632-1638.

Isaac, D.I., Golenberg, N., Haut, R.C. Acute repair of chondrocytes in the rabbit tibiofemoral joint following blunt impact using P188 surfactant and a preliminary investigation of its long-term efficacy. *Journal of Orthopaedic Research* (In Review).

Isaac, D.I., Meyer, E.G., Haut, R.C. (2008) Chondrocyte damage and contact pressures following impact on the rabbit tibiofemoral joint. *J Biomech Eng* **130,** 0410181-5.

Isaac, D.I. (2009) Chapter 5: Acute repair of chondrocytes in the rabbit tibiofemoral joint following blunt impact using P188 surfactant. In: *Investigations on the response of knee joint cartilage to blunt impact in a small animal model.* Thesis for the degree of M.S. Michigan State University, 79-101.

Kurz, B., Jin, M., Patwari, P., Cheng, D.M., Lark, M.W., Grodzinsky, A.J. (2001) Biosynthetic response and mechanical properties of articular cartilage after injurious compression. *J Orthop Res* **19,** 1140-1146.

Lane, N. (1996) Physical activity at leisure and risk of osteoarthritis. *Annals Rheumatic Disease* **55**, 682-684.

Levin, A., Burton-Wurster, N., Chen, C.T., Lust, G. (2001) Intercellular signaling as a cause of cell death in cyclically impacted cartilage explants. *Osteoarthritis and Cartilage* **9**, 702-711.

Majno, G., Joris, I. (1995) Apoptosis, oncosis and necrosis: an overview of cell death. *American Journal of Pathology* **146**, 3-15.

Marks, J.D., Pan, C.Y., Bushell, T., Cromie, W., Lee, R.C. (2001) Amphiphilic tri-block copolymers provide potent membrane-targeted neuroprotection. *FASEB* **15,** 1107-1109.

Natoli, R.M., Athanasiou, K.A. (2008) P188 reduces cell death and IGF-I reduces GAG release following single-impact loading of articular cartilage. *J Biomech Eng* **130,** 041012-1-9.

Rundell, S.A., Baars, D.C., Phillips, D.M., Haut, R.C. (2005) The limitation of acute necrosis in retro-patellar cartilage after a severe blunt impact to the in vivo rabbit patello-femoral joint. *J Orthop Res* **23,** 1363-1369.

Simon, W.H., Richardson, S., Herman, W., Parsons, J.R., Lane, J. (1976) Long-term effects of chondrocyte death on rabbit articular cartilage in vivo. *Journal of Bone and Joint Surgery, Am* **58,** 517-526.

Wilkins, R.J., Browning, J.A., Urban, J.P.G. (2000) Chondrocyte regulation by mechanical load. *Bioheology* **37,** 67-74.

Chapter 6

Conclusions and Recommendations for Future Work

The previous chapters described investigations on the mechanical and biological properties of articular cartilage following various loading conditions using a small animal model and chondral explants. Additionally, interventions using poloxamer 188 and glucosamine chondroitin sulfate were investigated following injury to the cartilage.

In Chapter 1, differences in the mechanical properties of the rabbit tibial plateau were documented between the medial and lateral facets, as well as in areas covered and uncovered by the meniscus. Histological differences were also documented between the medial and lateral facets. Additionally, surface fissuring and histologically identified matrix damage of articular cartilage were documented in the medial compartment that paralleled with reductions in fiber modulus and increases in permeability and tissue thickness in the medial versus lateral compartments of the plateau. These results suggest that in using the more complex model of cartilage, the mechanical properties in the model better defined the topographical mechanical properties of the joint and correlated well with the matrix components that had been previously suggested to regulate these parameters. Using the more complex fibril-reinforced biphasic model, future studies are still necessary to define the changes in tissue properties due to normal and abnormal loading of the joint.

Chapter 2 described investigations on the effects of 10 MPa and 25 MPa of unconfined compression on bovine chondral explants, as well as the effects of post-trauma treatment of the tissue with glucosamine-chondroitin sulfate. A significant decrease in the mechanical properties of the tissue was documented following 25 MPa of

unconfined compression compared to 10 MPa of unconfined compression. Treatment with glcN-CS resulted in an increase in the proteoglycan content and matrix stiffness for both 10 and 25 MPa of unconfined compression. Previous studies have documented the ability of cyclic loading and glcN-CS to increase PG content pre-trauma.

Cartilage explants were cyclically loaded following two levels of unconfined compression in Chapter 3. Additionally, glcN-CS treatment with cyclic loading was investigated. An increase in PG content was documented following cyclic loading and glcN-CS treatment following 10 and 25 MPa of unconfined compression compared to cyclic loading alone. Similar to the previous chapter, an increase in the matrix stiffness was also documented with glcN-CS treatment following 25 MPa of unconfined compression. However, following 10 MPa of unconfined compression and cyclic loading, no increase in the matrix stiffness was documented with the treatment of glcN-CS. This may be due to the size and binding sites of the proteoglycans in the matrix and its influence on the mechanical properties of the tissue. A comparison with Chapter 2 revealed no differences between the cyclically loaded and non-loaded explants following either level of unconfined compression. Future studies should investigate the cell viability and synthesis following unconfined compression with and without cyclic loading as well as the size and shape of the proteoglycans to further understand the effects of unconfined compression. This may lead to possible intervention methods and better treatments for the damaged cartilage.

Chapter 4 investigates the long-term efficacy of P188 following a traumatic injury to the rabbit tibio-femoral joint. A significant decrease in the density of viable cells was documented in the untreated limb versus the contralateral, control limb. This decrease

was not found in the treated animals. This would suggest a long term efficacy of P188. No visual signs of OA were documented in either the treated or untreated rabbit. Previous studies suggest that the visual appearance is not always a good indication of the integrity of the cartilage and that analysis of the mechanical properties are still necessary. Therefore, future studies should investigate the mechanical properties of the cartilage and the effects of saving the cells with P188 treatment.

These chapters investigate the changes in homeostasis of the cartilage constituents following traumatic injury and possible therapeutic treatments. This may provide a better understanding of the cause and pathways of OA. Future work may focus on these degenerative changes and a combination of these therapeutic treatments to develop better preventative and treatment methods of the OA patient in the long term.

Appendix A

Raw Data from Chapter 2

Table A.1 Mechanical properties of the control rabbits in site 1.

SITE 1 (CONTROLS) - MEDIAL UNCOVERED								
Specimen	h (mm)	e (%)	Em (Pa)	Ef (Pa)	k0 (Abaqus)	k0 (m^4/Ns)	k @ e=0.1	M
BU3L1	0.84	11.90	1.335E+06	3.815E+06	3.183E-10	3.245E-14	3.629E-11	70.197
BU3R1	0.90	11.11	1.587E+06	1.617E+06	1.382E-09	1.409E-13	4.475E-10	80.634
BU6L1	0.89	11.24	1.123E+06	3.585E+06	4.440E-10	4.526E-14	5.366E-11	70.780
BU6R1	0.96	10.42	1.006E+06	3.133E+06	7.106E-10	7.244E-14	7.062E-11	68.824
BU13L1	0.75	13.33	1.508E+06	1.913E+06	4.006E-10	4.084E-14	2.097E-12	39.387
BU13R1	0.87	11.49	8.776E+05	2.874E+06	4.706E-10	4.797E-14	3.480E-11	65.869
RK191L1	1.00	10.00	8.756E+05	3.337E+06	1.767E-10	1.801E-14	2.191E-11	71.041
RK191R1	0.95	10.53	8.322E+05	2.359E+06	1.158E-09	1.180E-13	3.046E-10	78.560
RKM82L1	0.88	11.36	9.288E+05	3.865E+06	8.315E-10	8.476E-14	2.329E-11	56.157
RKM82R1	0.84	11.90	1.022E+06	4.475E+06	3.477E-10	3.545E-14	3.698E-11	69.502
V36L1	0.94	10.64	5.553E+05	4.469E+06	5.002E-10	5.099E-14	6.174E-11	70.992
V36R1	0.92	10.87	6.607E+05	4.597E+06	4.329E-10	4.413E-14	2.710E-11	64.201
V38L1	0.80	12.50	1.054E+06	1.817E+06	4.116E-10	4.196E-14	1.114E-11	55.817
V38R1	0.80	12.50	1.182E+06	2.076E+06	8.825E-10	8.996E-14	9.901E-11	70.037
VAY3L1	0.82	12.20	1.943E+06	3.630E+06	3.307E-10	3.371E-14	5.241E-12	50.464
VAY3R1	0.68	14.71	2.222E+06	2.024E+06	1.809E-10	1.844E-14	8.164E-13	37.901
ZEM9L1	0.86	11.63	6.242E+05	4.133E+06	5.244E-10	5.346E-14	5.998E-11	70.228
ZEM9R1	0.90	11.11	7.676E+05	3.261E+06	5.702E-10	5.812E-14	6.121E-11	69.596
ZIA3C1	1.13	8.85	1.023E+06	7.193E+06	3.305E-10	3.369E-14	3.999E-11	70.790
Average	**0.88**	**11.49**	**1.112E+06**	**3.377E+06**	**5.476E-10**	**5.582E-14**	**7.358E-11**	**64.788**

Table A.2 Mechanical properties of the control rabbits in site 2.

SITE 2 (CONTROLS) - MEDIAL COVERED								
Specimen	**h (mm)**	**e (%)**	**Em (Pa)**	**Ef (Pa)**	**k0 (Abaqus)**	**k0 (m^4/Ns)**	**k @ e=0.1**	**M**
BU3L2	0.48	20.83	1.110E+06	1.460E+06	1.597E-10	1.628E-14	1.806E-13	24.062
BU3R2	0.54	18.52	1.543E+06	1.851E+06	1.389E-10	1.415E-14	3.705E-13	32.649
BU6L2	0.46	21.74	1.010E+06	1.368E+06	1.302E-10	1.327E-14	1.389E-13	23.479
BU6R2	0.61	16.39	1.106E+06	2.486E+06	2.112E-10	2.153E-14	1.105E-12	39.377
BU13L2	0.59	16.95	6.938E+05	2.089E+06	2.717E-10	2.769E-14	1.268E-12	38.237
BU13R2	0.47	21.28	5.743E+05	1.439E+06	3.276E-10	3.339E-14	4.622E-13	26.276
RK191L2	0.66	15.15	5.596E+05	1.767E+06	5.465E-10	5.571E-14	2.252E-11	60.020
RK191R2	0.92	10.87	5.930E+05	6.366E+06	1.985E-10	2.024E-14	2.564E-11	71.444
RKM82L2	0.49	20.41	9.096E+05	1.819E+06	2.550E-10	2.599E-14	4.345E-13	28.165
RKM82R2	0.55	18.18	1.024E+06	3.058E+06	2.407E-10	2.454E-14	7.190E-13	33.777
V36L2	0.67	14.93	1.370E+06	2.253E+06	2.231E-10	2.274E-14	1.879E-12	44.146
V36R2	0.60	16.67	8.217E+05	1.673E+06	2.780E-10	2.834E-14	2.350E-12	44.181
V38L2	0.60	16.67	6.357E+05	1.487E+06	4.717E-10	4.808E-14	2.313E-12	38.732
V38R2	0.54	18.52	5.100E+05	8.827E+05	8.980E-10	9.154E-14	1.438E-11	50.566
VAY3L2	0.52	19.23	1.291E+06	1.226E+06	2.979E-10	3.036E-14	6.905E-13	31.241
VAY3R2	0.42	23.81	1.344E+06	4.889E+06	3.474E-11	3.541E-15	1.861E-14	16.592
ZEM9L2	0.78	12.82	2.316E+05	5.049E+06	6.622E-10	6.750E-14	4.661E-11	65.375
ZEM9R2	0.66	15.15	5.121E+05	2.682E+06	1.008E-09	1.028E-13	2.834E-11	56.196
ZIA3C2	0.89	11.24	1.290E+06	7.998E+06	1.989E-10	2.028E-14	2.136E-11	69.597
Average	**0.60**	**17.33**	**9.015E+05**	**2.729E+06**	**3.449E-10**	**3.515E-14**	**8.988E-12**	**41.795**

Table A.3 Mechanical properties of the control rabbits in site 3.

SITE 3 (CONTROLS) - LATERAL UNCOVERED								
Specimen	**h (mm)**	**e (%)**	**Em (Pa)**	**Ef (Pa)**	**k0 (Abaqus)**	**k0 (m^4/Ns)**	**k @ e=0.1**	**M**
BU3L3	0.66	15.15	9.833E+05	2.721E+06	3.990E-10	4.068E-14	2.326E-12	40.463
BU3R3	0.60	16.67	1.165E+06	2.861E+06	1.948E-10	1.986E-14	5.045E-13	32.348
BU6L3	0.63	15.87	1.270E+06	6.272E+06	1.264E-10	1.289E-14	2.511E-13	29.698
BU6R3	0.69	14.49	1.215E+06	5.008E+06	1.625E-10	1.656E-14	5.432E-13	34.905
BU13L3	0.65	15.38	1.604E+06	4.978E+06	1.773E-10	1.808E-14	8.023E-13	37.929
BU13R3	0.59	16.95	1.483E+06	3.829E+06	1.501E-10	1.530E-14	3.290E-13	30.682
RK191L3	0.82	12.20	6.805E+05	3.160E+06	5.646E-10	5.755E-14	1.308E-11	54.259
RK191R3	0.85	11.76	6.800E+05	2.507E+06	1.432E-09	1.460E-13	1.166E-10	66.833
RKM82L3	0.54	18.52	1.126E+06	2.567E+06	3.085E-10	3.145E-14	8.119E-13	32.509
RKM82R3	0.40	25.00	8.116E+05	5.970E+06	8.335E-11	8.497E-15	6.914E-14	20.964
V36L3	0.68	14.71	1.458E+06	6.266E+06	2.142E-10	2.184E-14	1.365E-12	41.355
V36R3	0.80	12.50	1.048E+06	1.248E+07	2.748E-10	2.801E-14	3.584E-11	71.543
V38L3	0.66	15.15	7.840E+05	3.489E+06	3.559E-10	3.628E-14	4.786E-12	48.822
V38R3	0.52	19.23	7.588E+05	9.780E+05	1.019E-09	1.039E-13	2.696E-12	32.567
VAY3L3	0.54	18.52	1.557E+06	3.624E+06	3.138E-10	3.198E-14	9.054E-13	33.431
VAY3R3	0.48	20.83	1.073E+06	5.645E+06	1.250E-10	1.274E-14	2.385E-13	29.299
ZEM9L3	0.65	15.38	1.226E+06	7.967E+06	1.405E-10	1.433E-14	4.393E-13	34.232
ZEM9R3	0.66	15.15	1.066E+06	4.179E+06	3.240E-10	3.303E-14	1.931E-12	40.684
ZIA3C3	0.63	15.87	1.528E+06	4.254E+06	2.496E-10	2.544E-14	8.487E-13	35.073
Average	**0.63**	**16.28**	**1.132E+06**	**4.671E+06**	**3.482E-10**	**3.549E-14**	**9.704E-12**	**39.347**

Table A.4 Mechanical properties of the control rabbits in site 4.

SITE 4 (CONTROLS) - LATERAL COVERED								
Specimen	**h (mm)**	**e (%)**	**Em (Pa)**	**Ef (Pa)**	**k0 (Abaqus)**	**k0 (m^4/Ns)**	**k @ e=0.1**	**M**
BU3L4	0.48	10.42	4.022E+05	5.354E+07	5.637E-11	5.746E-15	4.829E-14	21.287
BU3R4	0.32	15.63	2.036E+05	1.691E+07	7.688E-11	7.837E-15	6.246E-14	20.756
BU6L4	0.32	15.63	2.153E+06	4.961E+07	1.223E-11	1.247E-15	1.121E-14	21.960
BU6R4	0.29	17.24	6.595E+05	6.606E+06	3.057E-10	3.116E-14	5.972E-13	29.531
BU13L4	0.31	16.13	3.481E+05	1.630E+07	1.643E-10	1.675E-14	1.754E-13	23.486
BU13R4	0.18	27.78	5.562E+05	5.382E+06	5.917E-11	6.031E-15	1.757E-14	10.692
RK191L4	0.42	11.90	2.274E+05	1.898E+07	2.215E-10	2.257E-14	4.340E-13	29.562
RK191R4	0.37	13.51	1.944E+05	1.540E+07	3.375E-10	3.440E-14	6.131E-13	28.804
RKM82L4	0.32	15.63	3.697E+05	2.948E+07	3.626E-11	3.696E-15	1.133E-14	11.202
RKM82R4	0.38	13.16	2.355E+05	3.729E+07	5.960E-11	6.075E-15	3.049E-14	16.132
V36L4	0.27	18.52	1.566E+06	8.161E+06	7.049E-11	7.186E-15	9.531E-14	25.851
V36R4	0.22	22.73	8.490E+05	9.220E+06	8.207E-11	8.366E-15	3.658E-14	14.754
V38L4	0.20	25.00	4.949E+04	8.654E+06	2.809E-10	2.863E-14	6.357E-14	7.976
V38R4	0.26	19.23	8.011E+05	2.379E+06	4.075E-10	4.154E-14	6.355E-13	27.278
VAY3L4	0.30	16.67	5.692E+05	3.897E+07	2.003E-11	2.042E-15	1.020E-14	16.088
VAY3R4	0.21	23.81	8.469E+05	1.395E+07	1.925E-11	1.962E-15	5.810E-15	10.853
ZEM9L4	0.20	25.00	6.551E+05	1.501E+07	1.162E-11	1.184E-15	3.142E-15	9.759
ZEM9R4	0.26	19.23	8.463E+05	1.932E+07	3.397E-11	3.463E-15	1.695E-14	15.881
ZIA3C4	0.20	25.00	3.324E+05	2.242E+07	1.278E-11	1.303E-15	2.293E-15	5.655
Average	**0.29**	**18.54**	**6.244E+05**	**2.040E+07**	**1.194E-10**	**1.217E-14**	**1.511E-13**	**18.290**

Appendix B

Raw Data from Chapter 3

Table B.1 Mechanical properties following 10 MPa of unconfined compression. Matrix Modulus (a) Fiber Modulus (b) Permeability (c).

10 MPa (E_m- % day 0)		
7	14	21
65.77	84.07	93.82
80.65	64.49	80.79
109.11	97.74	97.25
107.62		
64.91	77.51	58.89
66.08	72.23	95.14
56.01	94.68	52.31
69.36	78.86	102.44
103.83		
81.86		

a

10 MPa (E_f- % day 0)		
7	14	21
72.61	137.74	152.51
64.35	102.19	
183.92	137.34	
136.98	116.97	143.84
60.69	102.85	35.40
79.66	131.16	113.02
78.11	126.05	42.79
57.41	87.76	117.49
139.05		
110.92		
110.15		
101.26		

b

10 MPa (k_0- % day 0)		
7	14	21
169.29	181.00	128.19
176.53	214.06	135.96
84.02	170.06	124.67
74.38	114.93	88.91
138.95	95.47	224.55
95.68	146.75	117.70
213.21	116.24	
214.25	140.60	150.25
82.55		
76.76		
94.96		
127.68		

c

Table B.2 Mechanical properties following 25 MPa of unconfined compression. Matrix Modulus (a) Fiber Modulus (b) Permeability (c).

25 MPa (E_m- % day 0)		
7	14	21
43.05	40.67	39.23
63.15	55.52	57.55
57.86	45.85	46.61
62.88	42.15	74.35
44.55	61.24	54.57
82.11	58.82	90.83
80.95		
53.10		
96.22		

a

25 MPa (E_f- % day 0)		
7	14	21
222.13	221.15	
229.12	169.73	254.64
		214.61
101.90	90.40	227.60
104.49	167.30	139.95
165.12	207.97	153.74
179.33	82.03	181.82
124.96	117.65	107.97
89.26		
128.03		
70.87		

b

25 MPa (k_0- % day 0)		
7	14	21
	456.95	408.35
219.91	290.44	235.91
367.81	403.19	329.98
284.67		292.55
172.47	239.79	213.03
93.90	83.01	87.27
172.87	196.79	155.82
95.75	63.67	139.52
21.78		
137.82		
167.77		

c

Table B.3 Matrix Modulus following 10 MPa (a) and 25 MPa of unconfined compression with glcN-CS treatment.

10 MPa (E_m- % day 0)		
7	14	21
140.50		
131.09		
55.03		
89.60		
	60.20	
	86.47	
		121.33
		132.40
		136.60
123.93	109.27	88.59
100.12	102.09	117.17
117.59	131.87	100.85
119.56	175.88	73.15

25 MPa (E_m- % day 0)		
7	14	21
52.24		
108.13		
152.90		
	55.92	
	113.41	
	100.72	
	55.11	
		65.36
		41.53
		110.40
		160.23
50.64	44.67	39.01
81.96	69.67	85.95
77.47	84.18	104.33
126.13	144.82	99.18

Table B.4 Proteoglycan content with and without glcN-CS treatment.

Proteoglycan Content			
No glcN-CS		glcN-CS	
10 MPa	25 MPa	10 MPa	25 MPa
27.96	16.49	40.13	23.31
11.69	14.14	40.60	31.62
7.53	17.14	57.20	36.47
11.64	12.44	46.49	31.18
34.86	19.19	52.32	27.30
27.18	31.50	46.89	19.92
44.73	17.24	58.51	71.81
32.71	29.17	63.23	53.49

Appendix C

Raw Data from Chapter 4

Table C.1 Matrix modulus following unconfined compression and exercise.

10 MPa (E_m- % day 0)			25 MPa (E_m- % day 0)		
7	14	21	7	14	21
70.18	53.15	81.66	58.07	56.94	57.82
94.94	83.26	53.84	57.98	38.26	46.90
92.44	63.76	100.10	65.58	36.08	49.20
42.17	39.29	38.81	41.33	24.93	41.77
86.92	90.80	83.49	85.54	62.78	66.41
47.70	35.28	57.79	50.31	62.35	62.85
149.91		100.00	67.91	43.38	55.48
104.36	49.21	59.83	62.87	55.90	37.90
80.10			40.70		
84.04			47.66		
69.31			60.09		
50.36			37.58		

Table C.2 Matrix modulus following unconfined compression and exercise with glcN-CS treatment.

10 MPa (E_m- % day 0)			25 MPa (E_m- % day 0)		
7	14	21	7	14	21
96.70			49.57		
48.05			72.58		
60.09			87.95		
92.29				101.96	
	74.88			131.08	
	83.21			70.11	
		71.45			66.64
		62.14			117.50
		62.62	72.86	71.31	70.89
97.30	106.64	83.29	49.21	49.52	40.01
		77.81	112.34		104.07
46.69	42.54	121.91			
56.08	44.84	46.73			

Table C.3 Proteoglycan content with and without glcN-CS treatment.

Proteoglycan Content			
No glcN-CS		glcN-CS	
10 MPa	25 MPa	10 MPa	25 MPa
8.13	35.03	21.04	29.54
12.24	31.38	27.01	36.51
7.41	22.10	30.64	38.63
2.58	15.10	26.54	35.75
28.15	31.04	38.59	23.03
28.16	24.15	44.13	24.38
36.55	15.53	44.92	43.71
28.68	18.72	40.69	51.59

Appendix D

Raw Data from Chapter 5

Table D.1 Live cell density analysis of the P188 treated rabbits (cells/mm^2).

	P188							
	LFL	**LFM**	**LTL**	**LTM**	**RFL**	**RFM**	**RTL**	**RTM**
BF732	1749.29	1577.97	937.77		2200.14	1947.67	1334.51	1235.33
	1614.04	1487.80	1091.05		1776.35	1758.31	937.77	74.84
	1586.99		1289.43			1568.96	1217.29	973.83
Average	**1650.11**	**1532.89**	**1106.08**		**1988.24**	**1758.31**	**1163.19**	**761.33**
BF744	2064.89	1767.33	1496.82	820.55	2290.31	1054.99	1487.80	1145.16
	1767.33	1704.21	1469.77	775.46	1803.40	1370.58	1027.94	757.43
	1803.40	1577.97	1623.06	874.65		1397.63	1433.70	
Average	**1878.54**	**1683.17**	**1529.88**	**823.55**	**2046.86**	**1274.40**	**1316.48**	**951.29**
BF738	1559.94	1181.22	1226.31	1127.12	1307.46	1325.50	1145.16	856.61
	1641.09	1370.58	1740.28	757.43	1839.46	1154.17	1018.92	757.43
	1568.96	1316.48	1361.56	1181.22	1731.26	1253.36		1054.99
Average	**1589.99**	**1289.43**	**1442.72**	**1021.92**	**1626.06**	**1244.34**	**1082.04**	**889.68**

Table D.2 Live cell density analysis of the untreated rabbits (cells/mm^2).

	Control							
	LFL	**LFM**	**LTL**	**LTM**	**RFL**	**RFM**	**RTL**	**RTM**
TF43	1424.68	1235.33	1163.19	1469.77	1605.02	1803.40	1334.51	775.46
	1334.51	1136.14	1217.29	730.38	1695.19	1605.02	1100.07	640.21
	1343.53	1190.24	955.80			1596.01		
Average	**1367.58**	**1187.24**	**1112.09**	**1100.07**	**1650.11**	**1668.14**	**1217.29**	**707.83**
544	1713.23	1190.24	1199.26	766.44	1767.33	1379.60	1677.16	892.68
	1722.24	1000.89	1100.07	685.29	1668.14	1397.63	1397.63	685.29
						1298.45		
Average	**1717.74**	**1095.56**	**1149.67**	**725.87**	**1717.74**	**1358.56**	**1537.40**	**788.99**
53BRF	1325.50	1289.43	1217.29	1064.00	1388.62	1550.92	1109.09	1109.09
	1983.74	1442.72	1442.72	919.73	1641.09	1460.75	1009.90	892.68
	1532.89				1605.02			
Average	**1614.04**	**1366.07**	**1330.00**	**991.87**	**1544.91**	**1505.84**	**1059.50**	**1000.89**